Generation of focused, nonspherically decaying pulses of electromagnetic radiation

H. Ardavan
Institute of Astronomy, University of Cambridge, Madingley Road, Cambridge CB3 0HA, United Kingdom
(Received 26 January 1998; revised manuscript received 20 July 1998)

Periodic pulses of polarized electromagnetic radiation can be generated whose intensity diminishes with the distance R_P from their source like R_P^{-1} instead of R_P^{-2}. The source required is an extended charge with a rotating distribution pattern whose outer parts move with linear phase speeds exceeding the speed of light *in vacuo*. The coherence and beaming of the radiation in question stem from constructive interference of the emitted waves and formation of caustics. These processes take place at different distances from the source for different sets of waves, so that the propagating wave packets embodying the pulses are constantly dispersed and reconstructed out of other waves. [S1063-651X(98)05211-8]

PACS number(s): 03.40.Kf, 41.20.Jb, 42.25.−p, 97.60.Gb

I. INTRODUCTION

Bolotovskii and Ginzburg [1] and Bolotovskii and Bykov [2] have shown that the coordinated motion of aggregates of charged particles can give rise to extended electric charges and currents whose distribution patterns propagate with a phase speed exceeding the speed of light *in vacuo* and that, once created, such propagating charged patterns act as sources of the electromagnetic fields in precisely the same way as any other moving sources of these fields (see also [3] and [4]). That these sources travel faster than light is not, of course, in any way incompatible with the requirements of special relativity. The superluminally moving pattern is created by the coordinated motion of aggregates of subluminally moving particles.

In this paper we calculate the electromagnetic fields that are generated by an extended source of this type in the case where the charged pattern rotates about a fixed axis with a constant angular frequency. (The simpler case in which the superluminal source moves rectilinearly with a constant acceleration is analyzed in an appendix.) This calculation and its outcome shed light on a diverse set of problems.

The recently discovered solutions of the homogeneous wave equation referred to, *inter alia*, as nondiffracting radiation beams, focus wave modes, or electromagnetic missiles describe signals that propagate through space with unexpectedly slow rates of decay or spreading [5]. The potential practical significance of such signals is clearly enormous. The search for *physically realizable* sources of them, however, has so far remained unsuccessful [6]. Our calculation provides a concrete example of the sources that are currently looked for in this field by establishing a physically tenable *inhomogeneous* solution of Maxwell's equations with the same characteristics.

Investigation of the present emission process was originally motivated by the observational data on pulsars [7]. The radiation received from these celestial sources of radio waves consists of highly coherent pulses (with as high a brightness temperature as 10^{30} K) that recur periodically (with stable periods of the order of 1 sec). The intense magnetic field ($\sim 10^{12}$ G) of the central neutron star in a pulsar affects a coupling between the rotation of this star and that of the distribution pattern of the plasma surrounding it, so that the magnetospheric charges and currents in these objects are of the same type as those described above [8,9]. The effect responsible for the extreme degree of coherence of the observed emission from pulsars, therefore, may well be the violation of the inverse square law that is here predicted by our calculation. The present analysis is relevant also to the mathematically similar problem of the generation of acoustic radiation by supersonic propellers and helicopter rotors [10,11].

We begin, in Sec. II, by considering the waves that are emitted by an element of the superluminally rotating source from the standpoint of geometrical optics. Next we calculate the amplitudes of these waves, i.e., the Green's function for the problem, from the retarded potential (Sec. III). In Sec. IV we introduce the notion of and specify the bifurcation surface: the locus of source points that approach the observer along the radiation direction with the wave speed at the retarded time. Section V is then devoted to handling the singularities of the integrands of the radiation integrals that occur on the bifurcation surface: The electric and magnetic fields are given by the Hadamard finite parts of the divergent integrals that result from differentiating the retarded potential under the integral sign. In Sec. VI we give a descriptive account of the analyzed emission process in more physical terms.

There are also four appendixes: Appendix A, in which the asymptotic values of the Green's functions associated with various components of the fields are calculated; Appendix B, whose task is to point out that singularities would occur irrespective of which alternative form of the retarded potential we adopt; Appendix C, which is included to show that the time interval during which the contributions from a source element on the bifurcation surface are made is by many orders of magnitude longer than that in which these contributions are received; and Appendix D, which is concerned with rectilinearly moving accelerated sources with superluminal velocities. It emerges from the analysis in Appendix D that constructive interference of the emitted waves and formation of caustics occur, in the case of a short-lived source, only long after the waves have emanated from the source and then only for a finite period. During this period, the intensity of the propagating caustic that is generated by the rectilinearly moving source in question decays only like $R_P^{-2/3}$.

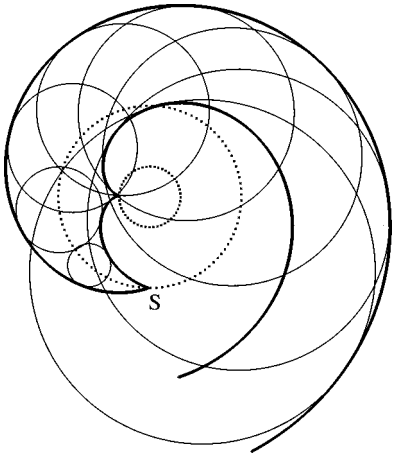

FIG. 1. Envelope of the spherical wave fronts emanating from a superluminally moving source point (S) in a circular motion. The heavier curves show the cross section of the envelope with the plane of the orbit of the source. The larger of the two dotted circles designates the orbit (at $r=3c/\omega$) and the smaller the light cylinder ($r_P=c/\omega$).

II. ENVELOPE OF THE WAVE FRONTS AND ITS CUSP

Consider a point source (an element of the propagating distribution pattern of a volume source) that moves on a circle of radius r with the constant angular velocity $\omega\hat{\mathbf{e}}_z$, i.e., whose path $\mathbf{x}(t)$ is given in terms of the cylindrical polar coordinates (r,φ,z), by

$$r=\text{const}, \quad z=\text{const}, \quad \varphi=\hat{\varphi}+\omega t, \tag{1}$$

where $\hat{\mathbf{e}}_z$ is the basis vector associated with z and $\hat{\varphi}$ the initial value of φ. The wave fronts that are emitted by this point source in an empty and unbounded space are described by

$$|\mathbf{x}_P-\mathbf{x}(t)|=c(t_P-t), \tag{2}$$

where the constant c denotes the wave speed and the coordinates $(\mathbf{x}_P,t_P)=(r_P,\varphi_P,z_P,t_P)$ mark the space-time of observation points. The distance R between the observation point $\mathbf{x}_P$ and a source point $\mathbf{x}$ is given by

$$|\mathbf{x}_P-\mathbf{x}|\equiv R(\varphi)=[(z_P-z)^2+r_P^2+r^2-2r_Pr\,\cos(\varphi_P-\varphi)]^{1/2}, \tag{3}$$

so that inserting Eq. (1) in Eq. (2) we obtain

$$R(t)\equiv[(z_P-z)^2+r_P^2+r^2-2r_Pr\,\cos(\varphi_P-\hat{\varphi}-\omega t)]^{1/2} =c(t_P-t). \tag{4}$$

These wave fronts are expanding spheres of radii $c(t_P-t)$ whose fixed centers ($r_P=r$, $\varphi_P=\hat{\varphi}+\omega t$, and $z_P=z$) depend on their emission times t (see Fig. 1).

Introducing the natural length scale of the problem c/ω and using $t=(\varphi-\hat{\varphi})/\omega$ to eliminate t in favor of φ, we can express Eq. (4) in terms of dimensionless variables as

$$g\equiv\varphi-\varphi_P+\hat{R}(\varphi)=\phi, \tag{5}$$

in which $\hat{R}\equiv R\omega/c$ and

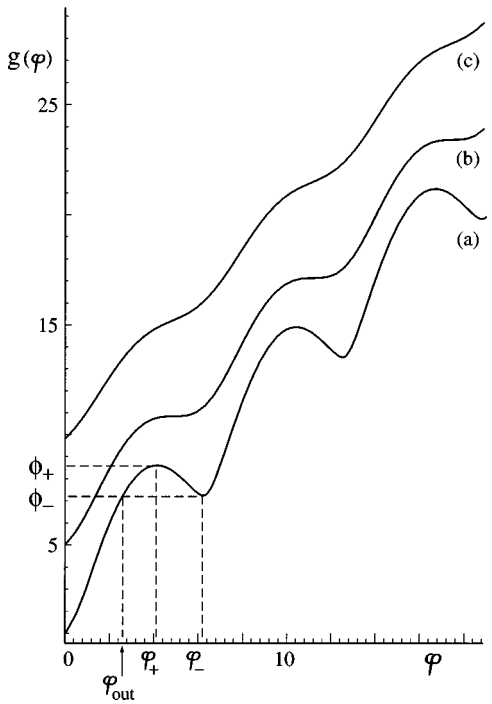

FIG. 2. Curve representing $g(\varphi)$ versus φ for $\varphi_P=0$, $\hat{r}_P=3$, $\hat{r}=2$, and (a) $\hat{z}=\hat{z}_P$, inside the bifurcation surface (the envelope), (b) $\hat{z}=\hat{z}_c$, on the cusp curve of the bifurcation surface (the envelope), and (c) $\hat{z}=2\hat{z}_c-\hat{z}_P$, outside the bifurcation surface (the envelope). The marked adjacent turning points of curve (a) have the coordinates $(\varphi_\pm,\phi_\pm)$ and φ_{out} represents the solution of $g(\varphi)=\phi_0$ for a ϕ_0 that tends to ϕ_- from below.

$$\phi\equiv\hat{\varphi}-\hat{\varphi}_P \tag{6}$$

stands for the difference between the positions $\hat{\varphi}=\varphi-\omega t$ of the source point and $\hat{\varphi}_P\equiv\varphi_P-\omega t_P$ of the observation point in the $(r,\hat{\varphi},z)$ space. The Lagrangian coordinate $\hat{\varphi}$ in Eq. (5) lies within an interval of length 2π (e.g., $-\pi<\hat{\varphi}\leq\pi$), while the angle φ, which denotes the azimuthal position of the source point at the retarded time t, ranges over $(-\infty,\infty)$.

Figure 1 depicts the wave fronts described by Eq. (5) for fixed values of $(r,\hat{\varphi},z)$ and ϕ (or t_P) and a discrete set of values of φ (or t). These wave fronts possess an envelope because when $r>c/\omega$ and so the speed of the source exceeds the wave speed, several wave fronts with differing emission times can pass through a single observation point simultaneously. Stated mathematically, for certain values of the coordinates $(r_P,\hat{\varphi}_P,z_P;r,z)$ the function $g(\varphi)$ shown in Fig. 2 is oscillatory and so can equal ϕ at more than one value of the retarded position φ: A horizontal line $\phi=\text{const}$ intersects curve (a) in Fig. 2 at either one or three points. Wave fronts become tangential to one another and so form an envelope at those points $(r_P,\hat{\varphi}_P,z_P)$ for which two roots of $g(\varphi)=\phi$ coincide. The equation describing this envelope can therefore be obtained by eliminating φ between $g=\phi$ and $\partial g/\partial\varphi=0$.

Thus the values of φ on the envelope of the wave fronts are given by

$$\partial g/\partial\varphi=1-\hat{r}\hat{r}_P\sin(\varphi_P-\varphi)/\hat{R}(\varphi)=0. \tag{7}$$

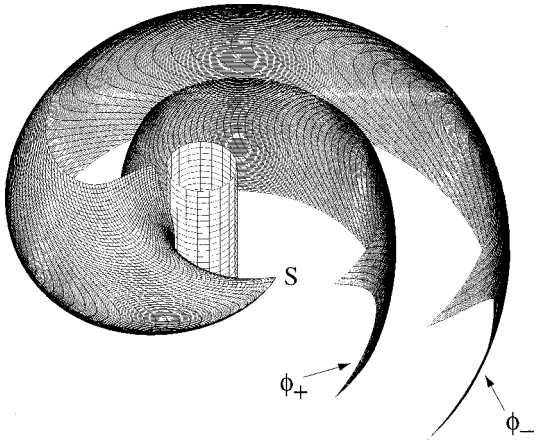

FIG. 3. Three-dimensional view of the light cylinder and the envelope of the wave fronts for the same source point (S) as that in Fig. 1 (only those parts of these surfaces that lie within the cylindrical volume $\hat{r}_P \leq 9$, $-2.25 \leq \hat{z}_P - \hat{z} \leq 2.25$ are shown). The two-sheeted tubelike surface constituting the envelope is symmetric with respect to the plane of the orbit and the cusp along which its sheets $\phi = \phi_\pm(r_P, z_P)$ meet is tangential to the light cylinder. For faster moving source points, the two sheets of the envelope intersect one another, as in Fig. 5.

When the curve representing $g(\varphi)$ is as in Fig. 2, curve (a) (i.e., $\hat{r} > 1$ and $\Delta > 0$), this equation has the doubly infinite set of solutions $\varphi = \varphi_\pm + 2n\pi$, where

$$\varphi_\pm = \varphi_P + 2\pi - \arccos[(1 \mp \Delta^{1/2})/(\hat{r}\hat{r}_P)], \tag{8}$$

$$\Delta \equiv (\hat{r}_P^2 - 1)(\hat{r}^2 - 1) - (\hat{z} - \hat{z}_P)^2, \tag{9}$$

n is an integer, and $(\hat{r}, \hat{z}; \hat{r}_P, \hat{z}_P)$ stand for the dimensionless coordinates $r\omega/c$, $z\omega/c$, $r_P\omega/c$, and $z_P\omega/c$, respectively. The function $g(\varphi)$ is locally maximum at $\varphi_+ + 2n\pi$ and minimum at $\varphi_- + 2n\pi$.

Inserting $\varphi = \varphi_\pm$ in Eq. (5) and solving the resulting equation for ϕ as a function of $(\hat{r}_P, \hat{z}_P)$, we find that the envelope of the wave fronts is composed of two sheets

$$\phi = \phi_\pm \equiv g(\varphi_\pm) = 2\pi - \arccos[(1 \mp \Delta^{1/2})/(\hat{r}\hat{r}_P)] + \hat{R}_\pm, \tag{10}$$

in which

$$\hat{R}_\pm \equiv [(\hat{z} - \hat{z}_P)^2 + \hat{r}^2 + \hat{r}_P^2 - 2(1 \mp \Delta^{1/2})]^{1/2} \tag{11}$$

are the values of $\hat{R}$ at $\varphi = \varphi_\pm$. For a fixed source point $(r, \hat{\varphi}, z)$, Eq. (10) describes a tubelike spiraling surface in the $(r_P, \hat{\varphi}_P, z_P)$ space of observation points that extends from the speed-of-light cylinder $\hat{r}_P = 1$ to infinity (see Figs. 1 and 3).

The two sheets $\phi = \phi_\pm$ of this envelope meet at a cusp. The cusp occurs along the curve

$$\phi = 2\pi - \arccos[1/(\hat{r}\hat{r}_P)] + (\hat{r}_P^2\hat{r}^2 - 1)^{1/2} \equiv \phi_c, \tag{12a}$$

$$\hat{z} = \hat{z}_P \pm (\hat{r}_P^2 - 1)^{1/2}(\hat{r}^2 - 1)^{1/2} \equiv \hat{z}_c, \tag{12b}$$

shown in Fig. 4, and constitutes the locus of points at which *three* different wave fronts intersect tangentially. On the cusp

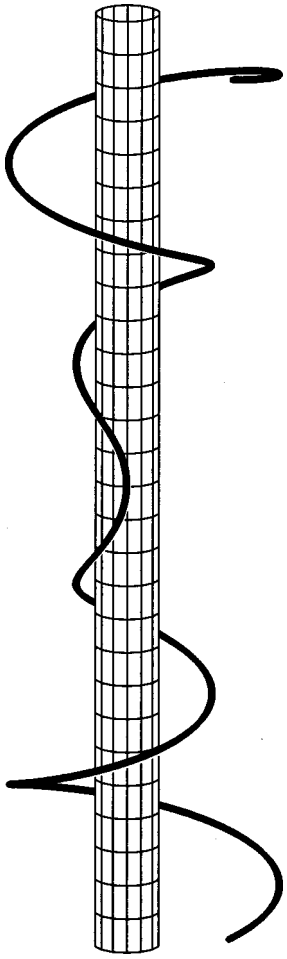

FIG. 4. Segment $-15 \leq \hat{z}_P - \hat{z} \leq 15$ of the cusp curve of the envelope shown in Fig. 3. This curve touches, and is tangential to, the light cylinder at the point ($\hat{r}_P = 1$, $\hat{z}_P = \hat{z}$ $\phi = \phi_c|_{\hat{r}_P = 1}$) on the plane of the orbit.

curve $\phi = \phi_c$, $z = z_c$, the function $g(\varphi)$ has a point of inflection [Fig. 2, curve (b)] and $\partial^2 g/\partial\varphi^2$, as well as $\partial g/\partial\varphi$ and g, vanishes at

$$\varphi = \varphi_P + 2\pi - \arccos[1/(\hat{r}\hat{r}_P)] \equiv \varphi_c. \tag{12c}$$

This, in conjunction with $t = (\varphi - \hat{\varphi})/\omega$, represents the common emission time of the three wave fronts that are mutually tangential at the cusp curve of the envelope.

In the highly superluminal regime, where $\hat{r} \gg 1$, the separation of the ordinates ϕ_+ and ϕ_- of adjacent maxima and minima in Fig. 2, curve (a), can be greater than 2π. A horizontal line $\phi = \text{const}$ will then intersect the curve representing $g(\varphi)$ at more than three points and so give rise to simultaneously received contributions that are made at 5, 7,..., distinct values of the retarded time. In such cases, the sheet ϕ_- of the envelope (issuing from the conical apex of this surface) undergoes a number of intersections with the sheet ϕ_+ before reaching the cusp curve (as in Fig. 5). We shall be concerned in this paper, however, mainly with source elements whose distances from the rotation axis do not appreciably exceed the radius c/ω of the speed-of-light cylinder and so for which the equation $g(\varphi) = \phi$ has at most three solutions.

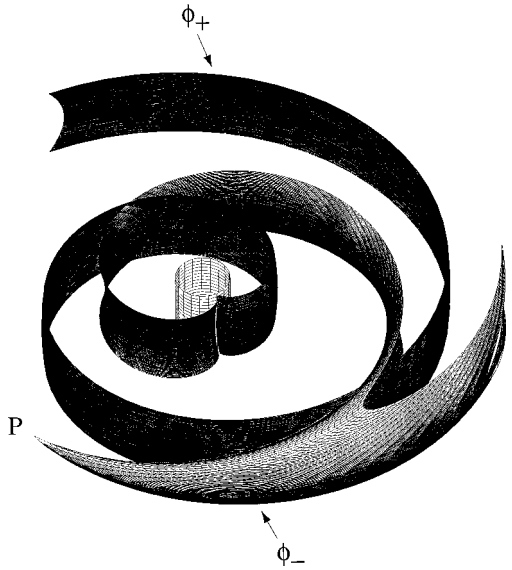

FIG. 5. Light cylinder and the bifurcation surface associated with the observation point P for a counterclockwise source motion. In this figure, P is located at $\hat{r}_P=9$ and only those parts of these surfaces that lie within the cylindrical volume $\hat{r}\leqslant 11$, $-1.5\leqslant \hat{z}-\hat{z}_P\leqslant 1.5$ are shown. The two sheets $\phi=\phi_\pm(r,z)$ of the bifurcation surface meet along a cusp (a curve of the same shape as that shown in Fig. 4) that is tangential to the light cylinder. For an observation point in the far zone ($\hat{r}_P\gg 1$), the spiraling surface that issues from P undergoes a large number of turns, in which its two sheets intersect one another, before reaching the light cylinder.

At points of tangency of their fronts, the waves that interfere constructively to form the envelope propagate normal to the sheets $\phi=\phi_\pm(r_P,z_P)$ of this surface, in the directions

$$\hat{\mathbf{n}}_\pm \equiv (c/\omega)\boldsymbol{\nabla}_P(\phi_\pm-\phi)=\hat{\mathbf{e}}_{r_P}[\hat{r}_P-\hat{r}_P^{-1}(1\mp\Delta^{1/2})]/\hat{R}_\pm + \hat{\mathbf{e}}_{\varphi_P}/\hat{r}_P+\hat{\mathbf{e}}_{z_P}(\hat{z}_P-\hat{z})/\hat{R}_\pm, \tag{13}$$

with the speed c. ($\hat{\mathbf{e}}_{r_P}$, $\hat{\mathbf{e}}_{\varphi_P}$, and $\hat{\mathbf{e}}_{z_P}$ are the unit vectors associated with the cylindrical coordinates r_P, φ_P, and z_P of the observation point, respectively.) Nevertheless, the resulting envelope is a rigidly rotating surface whose shape does not change with time: In the $(r_P,\hat{\varphi}_P,z_P)$ space, its conical apex is stationary at $(r,\hat{\varphi},z)$ and its form and dimensions only depend on the constant parameter $\hat{r}$.

The set of waves that superpose coherently to form a particular section of the envelope or its cusp therefore cannot be the same (i.e., cannot have the same emission times) at different observation times. The packet of focused waves constituting any given segment of the cusp curve of the envelope, for instance, is constantly dispersed and reconstructed out of other waves. This one-dimensional caustic would not be unlimited in its extent as shown in Fig. 4, unless the source is infinitely long lived: Only then would the duration of the source encompass the required intervals of emission time for every one of its constituent segments (cf. the similar caustic encountered in Appendix D).

III. AMPLITUDES OF THE WAVES GENERATED BY A POINT SOURCE

Our discussion has been restricted so far to the geometrical features of the emitted wave fronts. In this section we proceed to find the Lienard-Wiechert potential for these waves.

The scalar potential arising from an element of the moving volume source we have been considering is given by the retarded solution of the wave equation

$$\nabla'^2 G_0-\partial^2 G_0/\partial(ct')^2=-4\pi\rho_0, \tag{14a}$$

in which

$$\rho_0(r',\varphi',z',t')=\delta(r'-r)\,\delta(\varphi'-\omega t'-\hat{\varphi})\,\delta(z'-z)/r' \tag{14b}$$

is the density of a point source of unit strength with the trajectory (1). In the absence of boundaries, therefore, this potential has the value

$$G_0(\mathbf{x}_P,t_P)=\int d^3x'dt'\rho_0(\mathbf{x}',t') \times\delta(t_P-t'-|\mathbf{x}_P-\mathbf{x}'|/c)/|\mathbf{x}_P-\mathbf{x}'| \tag{15a}$$

$$=\int_{-\infty}^{+\infty}dt'\,\delta(t_P-t'-R(t')/c)/R(t'), \tag{15b}$$

where $R(t')$ is the function defined in Eq. (4) (see, e.g., [12]).

If we use Eq. (1) to change the integration variable t' in Eq. (15b) to φ and express the resulting integrand in terms of the quantities introduced in Eqs. (3), (5), and (6), we arrive at

$$G_0(r,r_P,\hat{\varphi}-\hat{\varphi}_P,z-z_P)=\int_{-\infty}^{+\infty}d\varphi\;\delta(g(\varphi)-\phi)/R(\varphi). \tag{16}$$

This can then be rewritten, by formally evaluating the integral, as

$$G_0=\sum_{\varphi=\varphi_j}\frac{1}{R|\partial g/\partial\varphi|}, \tag{17}$$

where the angles φ_j are the solutions of the transcendental equation $g(\varphi)=\phi$ in $-\infty<\varphi<+\infty$ and correspond, in conjunction with Eq. (1), to the retarded times at which the source point $(r,\hat{\varphi},z)$ makes its contribution towards the value of G_0 at the observation point $(r_P,\hat{\varphi}_P,z_P)$.

Equation (17) shows, in the light of Fig. 2, that the potential G_0 of a point source is discontinuous on the envelope of the wave fronts: If we approach the envelope from outside, the sum in Eq. (17) has only a single term and yields a finite value for G_0, but if we approach this surface from inside, two of the ϕ_j's coalesce at an extremum of g and Eq. (17) yields a divergent value for G_0. Approaching the sheet $\phi=\phi_+$ or ϕ_- of the envelope from inside this surface corresponds, in Fig. 2, to raising or lowering a horizontal line $\phi=\phi_0=$const, with $\phi_-\leqslant\phi_0\leqslant\phi_+$, until it intersects curve (a) of this figure at its maximum or minimum tangentially. At an observation point thus approached, the sum in Eq. (17) has three terms, two of which tend to infinity.

On the other hand, approaching a neighboring observation point just outside the sheet $\phi=\phi_-$ (say) of the envelope corresponds, in Fig. 2, to raising a horizontal line $\phi=\phi_0$

=const, with $\phi_0 \leqslant \phi_-$, towards a limiting position in which it tends to touch curve (*a*) at its minimum. As long as it has not yet reached the limit, such a line intersects curve (*a*) at one point only. The equation $g(\varphi)=\phi$ therefore has only a single solution $\varphi=\varphi_{\text{out}}$ in this case, which is different from both φ_+ and φ_- and so at which $\partial g/\partial\varphi$ is nonzero (see Fig. 2). The contribution that the source makes when located at $\varphi=\varphi_{\text{out}}$ is received by both observers, but the constructively interfering waves that are emitted at the two retarded positions approaching φ_- only reach the observer inside the envelope.

The function G_0 has an even stronger singularity at the cusp curve of the envelope. On this curve, all three of the φ_j's coalesce [Fig. 2, curve (*b*)] and each denominator in the expression in Eq. (17) both vanishes and has a vanishing derivative ($\partial g/\partial\varphi=\partial^2 g/\partial\varphi^2=0$).

There is a standard asymptotic technique for evaluating radiation integrals with coalescing critical points that describe caustics [13–15]. By applying this technique, which we have outlined in Appendix A, to the integral in Eq. (16), we can obtain a uniform asymptotic approximation to G_0 for small $|\phi_+-\phi_-|$, i.e., for points close to the cusp curve of the envelope where G_0 is most singular. The result is

$$G_0^{\text{in}} \sim 2c_1^{-2}(1-\chi^2)^{-1/2}[p_0\cos(\tfrac{1}{3}\arcsin\chi) - c_1 q_0 \sin(\tfrac{2}{3}\arcsin\chi)], \quad |\chi|<1, \tag{18}$$

and

$$G_0^{\text{out}} \sim c_1^{-2}(\chi^2-1)^{-1/2}[p_0\sinh(\tfrac{1}{3}\operatorname{arccosh}|\chi|) + c_1 q_0 \operatorname{sgn}(\chi)\sinh(\tfrac{2}{3}\operatorname{arccosh}|\chi|)], \quad |\chi|>1, \tag{19}$$

where c_1, p_0, q_0, and χ are the functions of (r,z) defined in Eqs. (A2), (A5), (A6), and (A10) and approximated in Eqs. (A23)–(A30). The superscripts ''in'' and ''out'' designate the values of G_0 inside and outside the envelope and the variable χ equals $+1$ and -1 on the sheets $\phi=\phi_+$ and ϕ_- of this surface, respectively.

The function G_0^{out} is indeterminate but finite on the envelope [cf. Eq. (A39)], whereas G_0^{in} diverges like $\sqrt{3}c_1^{-2}(p_0 \mp c_1 q_0)/(1-\chi^2)^{1/2}$ as $\chi\to\pm 1$. The singularity structure of G_0^{in} close to the cusp curve is explicitly exhibited by

$$G_0^{\text{in}} \sim \frac{2}{3^{1/6}}(\omega/c)(\hat{r}^2\hat{r}_P^2-1)^{-1/2}c_0^{1/2}(\hat{z}_c-\hat{z})^{1/2}/[c_0^3(\hat{z}_c-\hat{z})^3 - (\phi_c-\phi)^2]^{1/2}, \tag{20}$$

in which $0\leqslant\hat{z}_c-\hat{z}\ll 1$, $|\phi_c-\phi|\ll 1$, and

$$c_0 \equiv \frac{2}{3^{2/3}}(\hat{r}^2\hat{r}_P^2-1)^{-1}(\hat{r}_P^2-1)^{1/2}(\hat{r}^2-1)^{1/2} \tag{21}$$

[see Eqs. (18) and (A22)–(A26)]. It can be seen from expression (20) that both the singularity on the envelope (at which the quantity inside the square brackets vanishes) and the singularity at the cusp curve (at which $\hat{z}_c-\hat{z}$ and $\phi_c-\phi$ vanish) are integrable singularities.

The potential of a volume source, which is given by the superposition of the potentials G_0 of its constituent volume elements and so involves integrations with respect to $(r,\hat{\varphi},z)$, is therefore finite. Since they are created by the coordinated motion of aggregates of particles, the types of sources we have been considering cannot, of course, be pointlike [1,2]. It is only in the physically unrealizable case where a superluminal source is pointlike that its potential has the extended singularities described above.

In fact, not only is the potential of an extended superluminally moving source singularity free, but it decays in the far zone like the potential of any other source. The alternative form of the retarded solution to the wave equation $\nabla^2 A_0-\partial^2 A_0/\partial(ct)^2=-4\pi\rho$ [which may be obtained from (15a) by performing the integration with respect to time],

$$A_0=\int d^3x\ \rho(\mathbf{x},t_P-|\mathbf{x}-\mathbf{x}_P|/c)/|\mathbf{x}-\mathbf{x}_P|, \tag{22}$$

shows that if the density ρ of the source is finite and vanishes outside a finite volume, then the potential A_0 decays like $|\mathbf{x}_P|^{-1}$ as the distance $|\mathbf{x}_P-\mathbf{x}|\simeq|\mathbf{x}_P|$ of the observer from the source tends to infinity.

IV. THE BIFURCATION SURFACE OF AN OBSERVER

Let us now consider an *extended* source that rotates about the z axis with the constant angular frequency ω. The density of such a source, when it has a distribution with an unchanging pattern, is given by

$$\rho(r,\varphi,z,t)=\rho(r,\hat{\varphi},z), \tag{23}$$

where the Lagrangian variable $\hat{\varphi}$ is defined by $\varphi-\omega t$ as in Eq. (1) and ρ can be any function of $(r,\hat{\varphi},z)$ that vanishes outside a finite volume.

If we insert this density in the expression for the retarded scalar potential [12] and change the variables of integration from (r,φ,z,t) to $(r,\hat{\varphi},z,t)$, we obtain

$$A_0(\mathbf{x}_P,t_P)=\int d^3x\ dt\ \rho(\mathbf{x},t)\,\delta(t_P-t-|\mathbf{x}-\mathbf{x}_P|/c)/|\mathbf{x}-\mathbf{x}_P| \tag{24a}$$

$$=\int r\ dr\ d\hat{\varphi}\ dz\ \rho(r,\hat{\varphi},z) \times G_0(r,r_P,\hat{\varphi}-\hat{\varphi}_P,z-z_P), \tag{24b}$$

where G_0 is the function defined in Eq. (16) that represents the scalar potential of a corresponding point source. That the potential of the extended source in question is given by the superposition of the potentials of the moving source points that constitute it is an advantage that is gained by marking the space of source points with the natural coordinates $(r,\hat{\varphi},z)$ of the source distribution. This advantage is lost if we use any other coordinates (cf. Appendix B).

In Sec. III, where the source was pointlike, the coordinates $(r,\hat{\varphi},z)$ of the source point in $G_0(r,r_P,\hat{\varphi}-\hat{\varphi}_P,z-z_P)$ were held fixed and we were concerned with the behavior of this potential as a function of the coordinates $(r_P,\hat{\varphi}_P,z_P)$ of the observation point. When we superpose the potentials of the volume elements that constitute an ex-

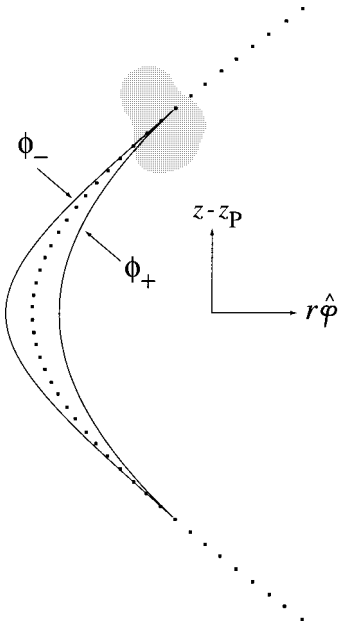

FIG. 6. Full curves depict the cross section, with the cylinder $\hat{r}=1.5$, of the bifurcation surface of an observer located at $\hat{r}_P=3$. (The motion of the source is counterclockwise.) The projection of the cusp curve of this bifurcation surface onto the cylinder $\hat{r}=1.5$ is shown as a dotted curve and the region occupied by the source as a dotted area. In this figure the observer's position is such that one of the points $(\phi=\phi_c,\ z=z_c)$ at which the cusp curve in question intersects the cylinder $\hat{r}=1.5$, the one with $z_c>0$, is located within the source distribution. As the radial position r_P of the observation point tends to infinity, the separation, at a finite distance z_c-z from (ϕ_c,z_c), of the shown cross sections decreases like $r_P^{-3/2}$.

tended source, on the other hand, the coordinates $(r_P,\hat{\varphi}_P,z_P)$ are held fixed and we are primarily concerned with the behavior of G_0 as a function of the integration variables $(r,\hat{\varphi},z)$.

Because G_0 is invariant under the interchange of $(r,\hat{\varphi},z)$ and $(r_P,\hat{\varphi}_P,z_P)$ if ϕ is at the same time changed to $-\phi$ [see Eqs. (5) and (16)], the singularity of G_0 occurs on a surface in the $(r,\hat{\varphi},z)$ space of source points that has the same shape as the envelope shown in Fig. 3 but issues from the fixed point $(r_P,\hat{\varphi}_P,z_P)$ and spirals around the z axis in the opposite direction to the envelope (see Fig. 5). In this paper we refer to this locus of singularities of G_0 as the *bifurcation surface* of the observation point P.

Consider an observation point P for which the bifurcation surface intersects the source distribution, as in Fig. 6. The envelope of the wave fronts emanating from a volume element of the part of the source that lies within this bifurcation surface encloses the point P, but P is exterior to the envelope associated with a source element that lies outside the bifurcation surface.

We have seen that three wave fronts, propagating in different directions, simultaneously pass an observer who is located inside the envelope of the waves emanating from a point source and only one wave front passes an observer outside this surface. Hence, in contrast to the source elements outside the bifurcation surface that influence the potential at P at only a single value of the retarded time, this potential receives contributions from each of the elements inside the bifurcation surface at *three* distinct values of the retarded time.

The elements inside but adjacent to the bifurcation surface, for which G_0 diverges, are sources of the constructively interfering waves that not only arrive at P simultaneously but also are emitted at the same (retarded) time. These source elements approach the observer along the radiation direction $\mathbf{x}_P-\mathbf{x}$ with the wave speed at the retarded time, i.e., are located at distances $R(t)$ from the observer for which

$$\left.\frac{dR}{dt}\right|_{t=t_P-R/c}=-c \tag{25}$$

[see Eqs. (4), (7), and (8)]. Their accelerations at the retarded time,

$$\left.\frac{d^2R}{dt^2}\right|_{t=t_P-R/c}=\mp\frac{c\omega\Delta^{1/2}}{\hat{R}_\pm}, \tag{26}$$

are positive on the sheet $\phi=\phi_-$ of the bifurcation surface and negative on $\phi=\phi_+$.

The source points on the *cusp curve* of the bifurcation surface, for which $\Delta=0$ and all three of the contributing retarded times coincide, approach the observer, according to Eq. (26), with zero acceleration as well as with the wave speed.

From a radiative point of view, the most effective volume elements of the superluminal source in question are those that approach the observer along the radiation direction with the wave speed and zero acceleration at the retarded time since the ratio of the emission to reception time intervals for the waves that are generated by these particular source elements generally exceeds unity by several orders of magnitude (see Appendix C). On each constituent ring of the source distribution that lies outside the light cylinder ($r=c/\omega$) in a plane of rotation containing the observation point there are two volume elements that approach the observer with the wave speed at the retarded time: one whose distance from the observer diminishes with positive acceleration and another for which this acceleration is negative. These two elements are closer to one another the smaller the radius of the ring. For the smallest of such constituent rings, i.e., for the one that lies on the light cylinder, the two volume elements in question coincide and approach the observer also with zero acceleration.

The other constituent rings of the source distribution (those on the planes of rotation that do not pass through the observation point) likewise contain two such elements if their radii are large enough for their velocity $r\omega\mathbf{e}_\varphi$ to have a component along the radiation direction equal to c. On the smallest possible ring in each plane, there is again a single volume element, at the limiting position of the two coalescing volume elements of the neighboring larger rings, that moves towards the observer not only with the wave speed but also with zero acceleration.

For any given observation point P, the efficiently radiating pairs of volume elements on various constituent rings of the source distribution collectively form a surface: the part of the bifurcation surface associated with P that intersects the source distribution. The locus of the coincident pairs of volume elements, which is tangential to the light cylinder at the point where it crosses the plane of rotation containing the

observer, constitutes the segment of the cusp curve of this bifurcation surface that lies within the source distribution.

Thus the bifurcation surface associated with any given observation point divides the volume of the source into two sets of elements with differing influences on the observed field. As in Eqs. (18) and (19), the potentials $G_0^{\rm in}$ and $G_0^{\rm out}$ of the source elements inside and outside the bifurcation surface have different forms: The boundary $|\chi(r,r_P,\hat{\varphi}-\hat{\varphi}_P,z-z_P)|=1$ between the domains of validity of Eqs. (18) and (19) delineates the envelope of wave fronts when the source point $(r,\hat{\varphi},z)$ is fixed and the coordinates $(r_P,\hat{\varphi}_P,z_P)$ of the observation point are variable and describes the bifurcation surface when the observation point $(r_P,\hat{\varphi}_P,z_P)$ is fixed and the coordinates $(r,\hat{\varphi},z)$ of the source point sweep a volume.

The expression (24b) for the scalar potential correspondingly splits into the following two terms when the observation point is such that the bifurcation surface intersects the source distribution:

$$A_0=\int dV\ \rho G_0 \tag{27a}$$

$$=\int_{V_{\rm in}} dV\ \rho G_0^{\rm in}+\int_{V_{\rm out}} dV\ \rho G_0^{\rm out}, \tag{27b}$$

where $dV\equiv r\ dr\ d\hat{\varphi}\ dz$, $V_{\rm in}$ and $V_{\rm out}$ designate the portions of the source that fall inside and outside the bifurcation surface (see Fig. 6), and $G_0^{\rm in}$ and $G_0^{\rm out}$ denote the different expressions for G_0 in these two regions. Note that the boundaries of the volume $V_{\rm in}$ depend on the position $(r_P,\hat{\varphi}_P,z_P)$ of the observer: The parameter $\hat{r}_P$ fixes the shape and size of the bifurcation surface and the position $(r_P,\hat{\varphi}_P,z_P)$ of the observer specifies the location of the conical apex of this surface. When the observation point is such that the cusp curve of the bifurcation surface intersects the source distribution, the volume $V_{\rm in}$ is bounded by $\phi=\phi_-$, $\phi=\phi_+$, and the part of the source boundary $\rho(r,\hat{\varphi},z)=0$ that falls within the bifurcation surface. The corresponding volume $V_{\rm out}$ is bounded by the same patches of the two sheets of the bifurcation surface and by the remainder of the source boundary.

In the vicinity of the cusp curve (12), i.e., for $|\phi_c-\phi|\ll 1$ and $0\leqslant\hat{z}_c-\hat{z}\ll 1$, the cross section of the bifurcation surface with a cylinder $\hat{r}=$const is described by

$$\begin{aligned}\phi_\pm-\phi_c\simeq&-(\hat{r}^2-1)^{1/2}(\hat{r}_P^2-1)^{1/2}(\hat{r}^2\hat{r}_P^2-1)^{-1/2}(\hat{z}_c-\hat{z})\\&\pm\frac{2^{3/2}}{3}(\hat{r}^2-1)^{3/4}(\hat{r}_P^2-1)^{3/4}\\&\times(\hat{r}_P^2\hat{r}^2-1)^{-3/2}(\hat{z}_c-\hat{z})^{3/2}\end{aligned} \tag{28}$$

[see Eqs. (10)–(12) and (A26)]. This cross section, which is shown in Fig. 6, has two branches meeting at the intersections of the cusp curve with the cylinder $\hat{r}=$const whose separation in ϕ, at a given $\hat{z}_c-\hat{z}$, diminishes like $\hat{r}_P^{-3/2}$ in the limit $\hat{r}_P\to\infty$. Thus, at finite distances $\hat{z}_c-\hat{z}$ from the cusp curve, the two sheets $\phi=\phi_-$ and ϕ_+ of the bifurcation surface coalesce and become coincident with the surface $\phi=\frac{1}{2}(\phi_-+\phi_+)\equiv c_2$ as $\hat{r}_P\to\infty$, that is to say, the volume $V_{\rm in}$ vanishes like $\hat{r}_P^{-3/2}$.

Because the dominant contributions towards the value of the radiation field come from those source elements that approach the observer, along the radiation direction, with the wave speed and zero acceleration at the retarded time, in what follows we shall be primarily interested in far-field observers, the cusp curves of whose bifurcation surfaces intersect the source distribution. For such observers, the Green's function $\lim_{\hat{r}_P\to\infty}G_0$ undergoes a jump discontinuity across the coalescing sheets of the bifurcation surface: The values of χ on the sheets $\phi=\phi_\pm$, and hence the functions $G_0^{\rm out}|_{\phi=\phi_-}$ and $G_0^{\rm out}|_{\phi=\phi_+}$, remain different even in the limit where $\phi=\phi_-$ and ϕ_+ coincide [cf. Eqs. (A10) and (A39)].

V. DERIVATIVES OF THE RADIATION INTEGRALS AND THEIR HADAMARD FINITE PARTS

A. Gradient of the scalar potential

In this section we begin the calculation of the electric and magnetic fields by finding the gradient of the scalar potential A_0, i.e., by calculating the derivatives of the integral in Eq. (27a) with respect to the coordinates (r_P,φ_P,z_P) of the observation point. If we regard its singular kernel G_0 as a classical function, then the integral in Eq. (27a) is improper and cannot be differentiated under the integral sign without characterizing and duly handling the singularities of its integrand. On the other hand, if we regard G_0 as a generalized function, then it would be mathematically permissible to interchange the orders of differentiation and integration when calculating $\boldsymbol{\nabla}_P A_0$.

This interchange results in a new kernel $\boldsymbol{\nabla}_P G_0$ whose singularities are nonintegrable. However, the theory of generalized functions prescribes a well-defined procedure for obtaining the physically relevant value of the resulting divergent integral, a procedure involving integration by parts that extracts the so-called Hadamard finite part of this integral [16]. Hadamard's finite part of the divergent integral representing $\boldsymbol{\nabla}_P A_0$ yields the value that we would have obtained if we had first evaluated the original integral for A_0 as an explicit function of $(r_P,\hat{\varphi}_P,z_P)$ and then differentiated it.

From the standpoint of the theory of generalized functions, therefore, differentiation of Eq. (27a) yields

$$\boldsymbol{\nabla}_P A_0=\int dV\ \rho\boldsymbol{\nabla}_P G_0=(\boldsymbol{\nabla}_P A_0)_{\rm in}+(\boldsymbol{\nabla}_P A_0)_{\rm out}, \tag{29a}$$

in which

$$(\boldsymbol{\nabla}_P A_0)_{\rm in,out}\equiv\int_{V_{\rm in,out}} dV\ \rho\boldsymbol{\nabla}_P G_0^{\rm in,out}. \tag{29b}$$

Since ρ vanishes outside a finite volume, the integral in Eq. (27a) extends over all values of $(r,\hat{\varphi},z)$ and so there is no contribution from the limits of integration towards the derivative of this integral.

The kernels $\boldsymbol{\nabla}_P G_0^{\rm in,out}$ of the above integrals may be obtained from Eq. (16). Applying $\boldsymbol{\nabla}_P$ to the right-hand side of

Eq. (16) and interchanging the orders of differentiation and integration, we obtain an integral representation of $\nabla_P G_0$ consisting of two terms: one arising from the differentiation of R that decays like r_P^{-2} as $r_P \to \infty$ and so makes no contribution to the field in the radiation zone and another that arises from the differentiation of the Dirac δ function and decays less rapidly than r_P^{-2}. For an observation point in the radiation zone, we may discard terms of the order of r_P^{-2} and write

$$\nabla_P G_0 \simeq (\omega/c) \int_{-\infty}^{+\infty} d\varphi \; R^{-1} \delta'(g-\phi)\hat{\mathbf{n}}, \quad \hat{r}_P \gg 1, \tag{30}$$

in which δ' is the derivative of the Dirac delta function with respect to its argument and

$$\hat{\mathbf{n}} \equiv \hat{\mathbf{e}}_{r_P}[\hat{r}_P - \hat{r}\,\cos(\varphi-\varphi_P)]/\hat{R} + \hat{\mathbf{e}}_{\varphi_P}/\hat{r}_P + \hat{\mathbf{e}}_{z_P}(\hat{z}_P - \hat{z})/\hat{R}. \tag{31}$$

Equation (30) yields $\nabla_P G_0^{\rm in}$ or $\nabla_P G_0^{\rm out}$ depending on whether ϕ lies within the interval (ϕ_-, ϕ_+) or outside it. If we now insert Eq. (30) in Eq. (29b) and perform the integrations with respect to $\hat{\varphi}$ by parts, we find that

$$(\nabla_P A_0)_{\rm in} \simeq (\omega/c) \int_S r\, dr\, dz \Bigg\{ -[\rho \mathbf{G}_1^{\rm in}]_{\phi=\phi_-}^{\phi=\phi_+} + \int_{\phi_-}^{\phi_+} d\phi \; \partial\rho/\partial\hat{\varphi} \; \mathbf{G}_1^{\rm in} \Bigg\}, \quad \hat{r}_P \gg 1, \tag{32}$$

and

$$(\nabla_P A_0)_{\rm out} \simeq (\omega/c) \int_S r\, dr\, dz \Bigg\{ [\rho \mathbf{G}_1^{\rm out}]_{\phi=\phi_-}^{\phi=\phi_+} + \left(\int_{-\pi}^{\phi_-} + \int_{\phi_+}^{+\pi} \right) d\phi \; \partial\rho/\partial\hat{\varphi} \; \mathbf{G}_1^{\rm out} \Bigg\}, \quad \hat{r}_P \gg 1, \tag{33}$$

in which S stands for the projection of $V_{\rm in}$ onto the (r,z) plane and $\mathbf{G}_1^{\rm in}$ and $\mathbf{G}_1^{\rm out}$ are given by the values of

$$\mathbf{G}_1 \equiv \int_{-\infty}^{+\infty} d\varphi \; R^{-1} \delta(g-\phi)\hat{\mathbf{n}} = \sum_{\varphi=\varphi_j} R^{-1} |\partial g/\partial\varphi|^{-1} \hat{\mathbf{n}} \tag{34}$$

for ϕ inside and outside the interval (ϕ_-, ϕ_+), respectively.

Like $G_0^{\rm in}$, the Green's function $\mathbf{G}_1^{\rm in}$ diverges on the bifurcation surface $\phi = \phi_\pm$, where $\partial g/\partial\varphi$ vanishes, but this singularity of $G_0^{\rm in}$ is integrable so that the value of the second integral in Eq. (32) is finite (see Sec. III and Appendix A). Hadamard's finite part of $(\nabla_P A_0)_{\rm in}$ (denoted by the prefix $\mathcal{F}$) is obtained by simply discarding those ''integrated'' or boundary terms in Eq. (32) that diverge (see [16]). Hence the physically relevant quantity $\mathcal{F}\{(\nabla_P A_0)_{\rm in}\}$ consists, in the far zone, of the volume integral in Eq. (32).

Let us choose an observation point for which the cusp curve of the bifurcation surface intersects the source distribution (see Fig. 6). When the dimensions ($\sim L$) of the source are negligibly smaller than those of the bifurcation surface (i.e., when $L \ll r_P$ and so $z_c - z \ll r_P$ throughout the source distribution) the functions $\mathbf{G}_1^{\rm in,out}$ in Eqs. (32) and (33) can be approximated by their asymptotic values (A34) and (A35) in the vicinity of the cusp curve (see Appendix A).

According to Eqs. (A34), (A36), and (A44), $\mathbf{G}_1^{\rm in}$ decays like $\mathbf{p}_1/c_1^2 = O(1)$ at points interior to the bifurcation surface where $\lim_{R_P \to \infty} \chi$ remains finite. Since the separation of the two sheets of the bifurcation surface diminishes like $\hat{r}_P^{-3/2}$ within the source [see Eq. (28)], it therefore follows that the volume integral in Eq. (32) is of the order of $\hat{r}_P^{-3/2}$, a result that can also be inferred from the far-field version of Eq. (A34) by explicit integration. Hence

$$\mathcal{F}\{(\nabla_P A_0)_{\rm in}\} = O(\hat{r}_P^{-3/2}), \quad \hat{r}_P \gg 1, \tag{35}$$

decays too rapidly to make any contribution towards the value of the electric field in the radiation zone.

Because $\mathbf{G}_1^{\rm out}$ is, in contrast to $\mathbf{G}_1^{\rm in}$, finite on the bifurcation surface, both the surface and the volume integrals on the right-hand side of Eq. (33) have finite values. Each component of the second term has the same structure as the expression for the potential itself and so decays like r_P^{-1} (see the ultimate paragraph of Sec. III). However, the first term, which would have canceled the corresponding boundary term in Eq. (32) and so would not have survived in the expression for $\nabla_P A_0$ had the Green's function $\mathbf{G}_1$ been continuous, behaves differently from any conventional contribution to a radiation field.

Insertion of Eq. (A39) in Eq. (33) yields the following expression for the asymptotic value of this boundary term in the limit where the observer is located in the far zone and the source is localized about the cusp curve of his or her bifurcation surface:

$$\int r\, dr\, dz [\rho \mathbf{G}_1^{\rm out}]_{\phi_-}^{\phi_+} \sim \tfrac{1}{3} c_1^{-2} \int r\, dr\, dz [\mathbf{p}_1 (\rho|_{\phi_+} - \rho|_{\phi_-}) + 2 c_1 \mathbf{q}_1 (\rho|_{\phi_+} + \rho|_{\phi_-})]. \tag{36}$$

In this limit, the two sheets of the bifurcation surface are essentially coincident throughout the domain of integration in Eq. (36) [see Eq. (28)]. So the difference between the values of the source density on these two sheets of the bifurcation surface is negligibly small ($\sim \hat{r}_P^{-3/2}$) for a smoothly distributed source and the functions $\rho|_{\phi_\pm}$ appearing in the integrand of Eq. (36) may correspondingly be approximated by their common limiting value $\rho_{\rm BS}(r,z)$ on these coalescing sheets.

Once the functions $\rho|_{\phi_\pm}$ are approximated by $\rho_{\rm BS}(r,z)$ and $\mathbf{q}_1$ by Eq. (A41), Eq. (36) yields an expression that can be written, to within the leading order in the far-field approximation $\hat{r}_P \gg 1$ [see Eqs. (A44) and (A45)], as

$$\int_S r\ dr\ dz[\rho \mathbf{G}_1^{\rm out}]_{\phi_-}^{\phi_+}$$

$$\sim 2^{3/2}(c/\omega)^2 \hat{r}_P^{-3/2}\int_{\hat{r}_<}^{\hat{r}_>} d\hat{r}(\hat{r}^2-1)^{-1/4}\mathbf{n}_1 \times \int_{\hat{z}_c - L_{\hat{z}}\omega/c}^{\hat{z}_c} d\hat{z}(\hat{z}_c-\hat{z})^{-1/2}\rho_{\rm BS}(r,z)$$

$$\sim 2^{5/2}(c/\omega)^2 \hat{r}_P^{-3/2}\int_{\hat{r}_<}^{\hat{r}_>} d\hat{r}(\hat{r}^2-1)^{-1/4}\mathbf{n}_1 (L_{\hat{z}}\omega/c)^{1/2}\langle \rho_{\rm BS}\rangle, \tag{37}$$

with

$$\langle \rho_{\rm BS}\rangle(r) \equiv \int_0^1 d\eta\ \rho_{\rm BS}(r,z)|_{z=z_c-\eta^2 L_{\hat{z}}}, \tag{38}$$

where $z_c - L_{\hat{z}}(r) \leqslant z \leqslant z_c$ and $r_< \leqslant r \leqslant r_>$ are the intervals over which the bifurcation surface intersects the source distribution (see Fig. 6). The quantity $\langle \rho_{\rm BS}\rangle(r)$ may be interpreted, at any given r, as a weighted average, over the intersection of the coalescing sheets of the bifurcation surface with the plane $z=z_c-\eta^2 L_{\hat{z}}$, of the source density ρ.

The right-hand side of Eq. (37) decays like $r_P^{-3/2}$ as $r_P \to \infty$. The second term in Eq. (33) thus dominates the first term in this equation and so the quantity $(\boldsymbol{\nabla}_P A_0)_{\rm out}$ itself decays like r_P^{-1} in the far zone.

B. Time derivative of the vector potential

Inasmuch as the charge density (23) has an unchanging distribution pattern in the $(r,\hat{\varphi},z)$ frame, the electric current density associated with the moving source we have been considering is given by

$$\mathbf{j}(\mathbf{x},t) = r\omega\rho(r,\hat{\varphi},z)\hat{\mathbf{e}}_\varphi, \tag{39}$$

in which $r\omega\hat{\mathbf{e}}_\varphi = r\omega[-\sin(\varphi-\varphi_P)\hat{\mathbf{e}}_{r_P} + \cos(\varphi-\varphi_P)\hat{\mathbf{e}}_{\varphi_P}]$ is the velocity of the element of the source pattern that is located at (r,φ,z). This current satisfies the continuity equation $\partial\rho/\partial(ct) + \boldsymbol{\nabla}\cdot\mathbf{j} = 0$ automatically.

In the Lorentz gauge, the retarded vector potential corresponding to Eq. (24a) has the form [12]

$$\mathbf{A}(\mathbf{x}_P,t_P) = c^{-1}\int d^3x\ dt\ \mathbf{j}(\mathbf{x},t) \times \delta(t_P - t - |\mathbf{x}-\mathbf{x}_P|/c)/|\mathbf{x}-\mathbf{x}_P|. \tag{40}$$

If we insert Eq. (39) in Eq. (40) and change the variables of integration from (r,φ,z,t) to $(r,\varphi,z,\hat{\varphi})$, as in Eq. (24), we obtain

$$\mathbf{A} = \int dV\ \hat{r}\rho(r,\hat{\varphi},z)\mathbf{G}_2(r,r_P,\hat{\varphi}-\hat{\varphi}_P,z-z_P), \tag{41}$$

in which $dV = r\ dr\ d\hat{\varphi}\ dz$, the vector $\mathbf{G}_2$, which plays the role of a Green's function, is given by

$$\mathbf{G}_2 \equiv \int_{-\infty}^{+\infty} d\varphi\ \hat{\mathbf{e}}_\varphi \delta(g(\varphi)-\phi)/R(\varphi) = \sum_{\varphi=\varphi_j} R^{-1}|\partial g/\partial\varphi|^{-1}\hat{\mathbf{e}}_\varphi, \tag{42}$$

and g and φ_j's are the same quantities as those appearing in Eq. (17) (see also Fig. 2).

Because Eqs. (17), (34), and (42) have the factor $|\partial g/\partial\varphi|^{-1}$ in common, the function $\mathbf{G}_2$ has the same singularity structure as those of G_0 and $\mathbf{G}_1$: It diverges on the bifurcation surface $\partial g/\partial\varphi = 0$ if this surface is approached from inside and it is most singular on the cusp curve of the bifurcation surface where in addition $\partial^2 g/\partial\varphi^2 = 0$. It is, moreover, described by two different expressions $\mathbf{G}_2^{\rm in}$ and $\mathbf{G}_2^{\rm out}$ inside and outside the bifurcation surface whose asymptotic values in the neighborhood of the cusp curve have exactly the same functional forms as those found in Eqs. (18) and (19), the only difference being that p_0 and q_0 in these expressions are replaced by the $\mathbf{p}_2$ and $\mathbf{q}_2$ given in Eq. (A37) (see Appendix A).

As in Eq. (29), therefore, the time derivative of the vector potential has the form $\partial\mathbf{A}/\partial t_P = (\partial\mathbf{A}/\partial t_P)_{\rm in} + (\partial\mathbf{A}/\partial t_P)_{\rm out}$, with

$$(\partial\mathbf{A}/\partial t_P)_{\rm in,out} \equiv -\omega\int_{V_{\rm in,out}} dV\ \hat{r}\rho\partial\mathbf{G}_2^{\rm in,out}/\partial\hat{\varphi}_P, \tag{43}$$

when the observation point is such that the bifurcation surface intersects the source distribution.

The functions $\mathbf{G}_2^{\rm in,out}$ depend on $\hat{\varphi}_P$ and $\hat{\varphi}$ in the combination $\hat{\varphi}-\hat{\varphi}_P$ only. We can therefore replace $\partial/\partial\hat{\varphi}_P$ in Eq. (43) by $-\partial/\partial\hat{\varphi}$ and perform the integration with respect to $\hat{\varphi}$ by parts to arrive at

$$(\partial\mathbf{A}/\partial t_P)_{\rm in} = c\int_S dr\ dz\ \hat{r}^2\left\{[\rho\mathbf{G}_2^{\rm in}]_{\phi=\phi_-}^{\phi=\phi_+} - \int_{\phi_-}^{\phi_+} d\phi\ \partial\rho/\partial\hat{\varphi}\ \mathbf{G}_2^{\rm in}\right\} \tag{44}$$

and

$$(\partial\mathbf{A}/\partial t_P)_{\rm out} = -c\int_S dr\ dz\ \hat{r}^2\left\{[\rho\mathbf{G}_2^{\rm out}]_{\phi=\phi_-}^{\phi=\phi_+} + \left(\int_{-\pi}^{\phi_-} + \int_{\phi_+}^{+\pi}\right) d\phi\ \partial\rho/\partial\hat{\varphi}\ \mathbf{G}_2^{\rm out}\right\}. \tag{45}$$

For the same reasons as those given in the paragraphs following Eqs. (32) and (33), Hadamard's finite part of $(\partial\mathbf{A}/\partial t_P)_{\rm in}$ consists of the volume integral in Eq. (44) and is of the order of $\hat{r}_P^{-3/2}$ [note that, according to Eqs. (A37) and (A42), $\mathbf{p}_2 \gg c_1\mathbf{q}_2$ and $\mathbf{p}_2/c_1^2 = O(1)$]. The volume integral in Eq. (45), moreover, decays like $\hat{r}_P^{-1}$, as does its counterpart in Eq. (33).

The part of $\partial\mathbf{A}/\partial t_P$ that decays more slowly than conventional contributions to a radiation field is the boundary term in Eq. (45). The asymptotic value of this term is given by an expression similar to that appearing in Eq. (36), except that

$\mathbf{p}_1$ and $\mathbf{q}_1$ are replaced by $\mathbf{p}_2$ and $\mathbf{q}_2$. Once the quantities $\rho|_{\phi_\pm}$ and $\mathbf{q}_2$ in the expression in question are approximated by $\rho_{\rm BS}$ and Eq. (A42), as before, it follows that

$$(\partial\mathbf{A}/\partial t_P)_{\rm out}\sim -c\int_S dr\ dz\ \hat r^2[\rho\mathbf{G}_2^{\rm out}]_{\phi_-}^{\phi_+}$$
$$\sim -\frac{4}{3}\,c\int_S dr\ dz\ \hat r^2\rho_{\rm BS}c_1^{-1}\mathbf{q}_2$$
$$\sim -\frac{2^{5/2}}{3}\,(c^2/\omega)\hat r_P^{-1/2}\hat{\mathbf{e}}_{\varphi_P}\int_{\hat r_<}^{\hat r_>}d\hat r\ \hat r^2$$
$$\times(\hat r^2-1)^{-1/4}\int_{\hat z_c-L_{\hat z}\omega/c}^{\hat z_c}d\hat z(\hat z_c-\hat z)^{-1/2}\rho_{\rm BS}. \tag{46}$$

This behaves like $\hat r_P^{-1/2}$ as $\hat r_P\to\infty$ since the $\hat z$ quadrature in Eq. (46) has the finite value $2(L_{\hat z}\omega/c)^{1/2}\langle\rho_{\rm BS}\rangle$ in this limit [see Eq. (37) and the text following it]. Hence the electric field vector of the radiation

$$\mathbf{E}=-\boldsymbol{\nabla}_P A_0-\partial\mathbf{A}/\partial(ct_P)\sim -c^{-1}(\partial\mathbf{A}/\partial t_P)_{\rm out}$$
$$\sim\frac{2^{7/2}}{3}\,(c/\omega)\hat r_P^{-1/2}\hat{\mathbf{e}}_{\varphi_P}\int_{\hat r_<}^{\hat r_>}d\hat r\ \hat r^2(\hat r^2-1)^{-1/4}(L_{\hat z}\omega/c)^{1/2}\langle\rho_{\rm BS}\rangle \tag{47}$$

itself decays like $r_P^{-1/2}$ in the far zone: As we have already seen in Sec. V A, the term $\boldsymbol{\nabla}_P A_0$ has the conventional rate of decay r_P^{-1} and so is negligible relative to $(\partial\mathbf{A}/\partial t_P)_{\rm out}$.

C. Curl of the vector potential

There are no contributions from the limits of integration towards the curl of the integral in Eq. (41) because ρ vanishes outside a finite volume and so the integral in this equation extends over all values of $(r,\hat\varphi,z)$. Hence differentiation of Eq. (41) yields

$$\mathbf{B}=\boldsymbol{\nabla}_P\times\mathbf{A}=\mathbf{B}_{\rm in}+\mathbf{B}_{\rm out}, \tag{48a}$$

in which

$$\mathbf{B}_{\rm in,out}\equiv\int_{V_{\rm in,out}}dV\ \hat r\rho\boldsymbol{\nabla}_P\times\mathbf{G}_2^{\rm in,out}. \tag{48b}$$

Operating with $\boldsymbol{\nabla}_P\times$ on the first member of Eq. (42) and ignoring the term that decays like r_P^{-2}, as in Eq. (30), we find that the kernels $\boldsymbol{\nabla}_P\times\mathbf{G}_2^{\rm in}$ and $\boldsymbol{\nabla}_P\times\mathbf{G}_2^{\rm out}$ of Eq. (48b) are given, in the radiation zone, by the values of

$$\boldsymbol{\nabla}_P\times\mathbf{G}_2\simeq(\omega/c)\int_{-\infty}^{+\infty}d\varphi\ R^{-1}\delta'(g-\phi)\hat{\mathbf{n}}\times\hat{\mathbf{e}}_\varphi,\quad \hat r_P\gg 1, \tag{49}$$

for ϕ inside and outside the interval (ϕ_-,ϕ_+), respectively. [$\hat{\mathbf{n}}$ is the unit vector defined in Eq. (31).]

Insertion of Eq. (49) in Eq. (48) now yields expressions whose $\hat\varphi$ quadratures can be evaluated by parts to arrive at

$$\mathbf{B}_{\rm in}\simeq\int_S dr\ dz\ \hat r^2\Big\{-[\rho\mathbf{G}_3^{\rm in}]_{\phi=\phi_-}^{\phi=\phi_+}$$
$$+\int_{\phi_-}^{\phi_+}d\phi\ \partial\rho/\partial\hat\varphi\ \mathbf{G}_3^{\rm in}\Big\},\quad \hat r_P\gg 1, \tag{50}$$

and

$$\mathbf{B}_{\rm out}\simeq\int_S dr\ dz\ \hat r^2\Big\{[\rho\mathbf{G}_3^{\rm out}]_{\phi=\phi_-}^{\phi=\phi_+}$$
$$+\Big(\int_{-\pi}^{\phi_-}+\int_{\phi_+}^{+\pi}\Big)d\phi\ \partial\rho/\partial\hat\varphi\ \mathbf{G}_3^{\rm out}\Big\},\quad \hat r_P\gg 1, \tag{51}$$

where $\mathbf{G}_3^{\rm in}$ and $\mathbf{G}_3^{\rm out}$ stand for the values of

$$\mathbf{G}_3\equiv\int_{-\infty}^{+\infty}d\varphi\ R^{-1}\delta(g-\phi)\hat{\mathbf{n}}\times\hat{\mathbf{e}}_\varphi$$
$$=\sum_{\varphi=\varphi_j}R^{-1}|\partial g/\partial\varphi|^{-1}\hat{\mathbf{n}}\times\hat{\mathbf{e}}_\varphi \tag{52}$$

inside and outside the bifurcation surface. Once again, owing to the presence of the factor $|\partial g/\partial\varphi|^{-1}$ in $\mathbf{G}_3^{\rm in}$, the first term in Eq. (50) is divergent so that the Hadamard finite part of $\mathbf{B}_{\rm in}$ consists of the volume integral in this equation, an integral whose magnitude is of the order of $\hat r_P^{-3/2}$ [see the paragraph containing Eq. (35) and note that, according to Eqs. (A38) and (A44), $\mathbf{p}_3\gg c_1\mathbf{q}_3$ and $\mathbf{p}_3/c_1^2=O(1)$]. The second term in Eq. (51) has, like those in Eqs. (33) and (45), the conventional rate of decay $\hat r_P^{-1}$. Moreover, the surface integral in Eq. (51), which would have had the same magnitude as the surface integral in Eq. (50) and so would have canceled out of the expression for $\mathbf{B}$ had $\mathbf{G}_3^{\rm in}$ and $\mathbf{G}_3^{\rm out}$ matched smoothly across the bifurcation surface, decays as slowly as the corresponding term in Eq. (45).

The asymptotic value of $\mathbf{G}_3$ for source points close to the cusp curve of the bifurcation surface has been calculated in Appendix A. It follows from this value of $\mathbf{G}_3$ and from Eqs. (51), (52), (A40), (A44), and (A45) that, in the radiation zone,

$$\mathbf{B}\sim\int_S dr\ dz\ \hat r^2[\rho\mathbf{G}_3^{\rm out}]_{\phi_-}^{\phi_+}\sim\frac{4}{3}\int_S dr\ dz\ \hat r^2\rho_{\rm BS}c_1^{-1}\mathbf{q}_3$$
$$\sim\frac{2^{5/2}}{3}\,(c/\omega)\hat r_P^{-1/2}\int_{\hat r_<}^{\hat r_>}d\hat r\ \hat r^2(\hat r^2-1)^{-1/4}$$
$$\times\int_{\hat z_c-L_{\hat z}\omega/c}^{\hat z_c}d\hat z(\hat z_c-\hat z)^{-1/2}\rho_{\rm BS}\mathbf{n}_3 \tag{53}$$

to within the order of the approximation entering Eqs. (37) and (46).

The far-field version of the radial unit vector defined in Eq. (31) assumes the form

$$\lim_{r_P\to\infty}\hat{\mathbf{n}}|_{\phi=\phi_c,\hat z=\hat z_c}=\hat r^{-1}\hat{\mathbf{e}}_{r_P}-(1-\hat r^{-2})^{1/2}\hat{\mathbf{e}}_{z_P} \tag{54}$$

on the cusp curve of the bifurcation surface [see Eqs. (12b), (13), and (A27) and note that the position of the observer is here assumed to be such that the segment of the cusp curve lying within the source distribution is described by the expression with the plus sign in Eq. (12b), as in Fig. 6]. So $\mathbf{n}_3$ equals $\hat{\mathbf{n}}\times\hat{\mathbf{e}}_{\varphi_P}$ in the regime of validity of Eq. (53) [see Eq. (A45)]. Moreover, $\hat{\mathbf{n}}$ can be replaced by its far-field value

$$\hat{\mathbf{n}}\simeq(r_P\hat{\mathbf{e}}_{r_P}+z_P\hat{\mathbf{e}}_{z_P})/R_P, \quad R_P\to\infty, \tag{55}$$

if it is borne in mind that Eq. (53) holds true only for an observer, the cusp curve of whose bifurcation surface intersects the source distribution.

Once $\mathbf{n}_3$ in Eq. (53) is approximated by $\hat{\mathbf{n}}\times\hat{\mathbf{e}}_{\varphi_P}$ and the resulting $\hat{z}$ quadrature is expressed in terms of $\langle\rho_{\rm BS}\rangle$ [see Eq. (38)], this equation reduces to

$$\mathbf{B}\sim\hat{\mathbf{n}}\times\mathbf{E}, \tag{56}$$

where $\mathbf{E}$ is the electric field vector earlier found in Eq. (47). Equations (47) and (56) jointly describe a radiation field whose polarization vector lies along the direction of motion of the source $\hat{\mathbf{e}}_{\varphi_P}$.

Note that there has been no contribution toward the values of $\mathbf{E}$ and $\mathbf{B}$ from inside the bifurcation surface. These quantities have arisen in the above calculation solely from the jump discontinuities in the values of the Green's functions $\mathbf{G}_1^{\rm out}$, $\mathbf{G}_2^{\rm out}$, and $\mathbf{G}_3^{\rm out}$ across the coalescing sheets of the bifurcation surface. We would have obtained the same results had we simply excised the vanishingly small volume $\lim_{r_P\to\infty}V_{\rm in}$ from the domains of integration in Eqs. (29), (43), and (48).

Note also that the way in which the familiar relation (56) has emerged from the present analysis is altogether different from that in which it appears in conventional radiation theory. Essential though it is to the physical requirement that the directions of propagation of the waves and of their energy should be the same, Eq. (56) expresses a relationship between fields that are here given by nonspherically decaying surface integrals rather than by the conventional volume integrals that decay like r_P^{-1}.

VI. CONCLUSION: A PHYSICAL DESCRIPTION OF THE EMISSION PROCESS

Expressions (47) and (56) for the electric and magnetic fields of the radiation that arises from a charge-current density with the components (23) and (39) imply the Poynting vector

$$\mathbf{S}\sim\frac{2^5}{3^2}\,\pi^{-1}c(c/\omega)^2\hat{r}_P^{-1}\left[\int_{\hat{r}_<}^{\hat{r}_>}d\hat{r}\;\hat{r}^2(\hat{r}^2-1)^{-1/4}\times(L_{\hat{z}}\omega/c)^{1/2}\langle\rho_{\rm BS}\rangle\right]^2\hat{\mathbf{n}}. \tag{57}$$

In contrast, the magnitude of the Poynting vector for the *coherent* cyclotron radiation that would be generated by a macroscopic lump of charge, if it moved subluminally with a centripetal acceleration $c\omega$, is of the order of $(\langle\rho\rangle L^3)^2\omega^2/(cR_P^2)$ according to the Larmor formula, where L^3 represents the volume of the source and $\langle\rho\rangle$ its average charge density. The intensity of the present emission is therefore greater than that of even a coherent conventional radiation by a factor of the order of $(L_{\hat{z}}/L)(L\omega/c)^{-4}(R_P/L)$, a factor that ranges from 10^{16} to 10^{30} in the case of pulsars for instance.

The reason this ratio has so large a value in the far field $(R_P/L\gg1)$ is that the radiative characteristics of a volume-distributed source that moves faster than the waves it emits are radically different from those of a corresponding source that moves more slowly than the waves it emits. There are source elements in the former case that approach the observer along the radiation direction with the wave speed at the retarded time. These lie on the intersection of the source distribution with what we have here called the bifurcation surface of the observer (see Figs. 5 and 6): a surface issuing from the position of the observer that has the same shape as the envelope of the wave fronts emanating from a source element (Figs. 1 and 3) but that spirals around the rotation axis in the opposite direction to this envelope and resides in the space of source points instead of the space of observation points.

The source elements inside the bifurcation surface of an observer make their contributions towards the observed field at three distinct instants of the retarded time. The values of two of these retarded times coincide for an interior source element that lies next to the bifurcation surface. This limiting value of the coincident retarded times represents the instant at which the component of the velocity of the source point in question equals the wave speed c in the direction of the observer. The third retarded time at which a source point adjacent to, just inside, the bifurcation surface makes a contribution is the same as the single retarded time at which its neighboring source element just outside the bifurcation surface makes its contribution towards the observed field. (The source elements outside the bifurcation surface make their contributions at only a single instant of the retarded time.)

At the instant marked by this third value of the retarded time, the two neighboring source elements, just interior and just exterior to the bifurcation surface, have the same velocity, but a velocity whose component along the radiation direction is different from c. The velocities of these two neighboring elements are, of course, equal at any time. However, at the time they approach the observer with the wave speed, the element inside the bifurcation surface makes a contribution towards the observed field while the one outside this surface does not: The observer is located just inside the envelope of the wave fronts that emanate from the interior source element but just outside the envelope of the wave fronts that emanate from the exterior one. Thus the constructive interference of the waves that are emitted by the source element just outside the bifurcation surface takes place along a caustic that at no point propagates past the observer at the conical apex of the bifurcation surface in question.

On the other hand, the radiation effectiveness of a source element that approaches the observer with the wave speed at the retarded time is much greater than that of a neighboring element, the component of whose velocity along the radiation direction is subluminal or superluminal at this time. This is because the piling up of the emitted wave fronts along the line joining the source and the observer makes the ratio of

emission to reception time intervals for the contributions of the luminally moving source elements by many orders of magnitude greater than that for the contributions of any other elements (see Appendix C). As a result, the radiation effectiveness of the various constituent elements of the source (i.e., the Green's function for the emission process) undergoes a discontinuity across the boundary set by the bifurcation surface of the observer.

The integral representing the superposition of the contributions of the various volume elements of the source to the potential thus entails a discontinuous integrand. When this volume integral is differentiated to obtain the field, the discontinuity in question gives rise to a boundary contribution in the form of a surface integral over its locus. This integral receives contributions from opposite faces of each sheet of the bifurcation surface that do not cancel one another. Moreover, the contributions arising from the exterior faces of the two sheets of the bifurcation surface do not have the same value even in the limit $R_P \to \infty$ where this surface is infinitely large and so its two sheets are, throughout a localized source that intersects the cusp, coalescent. Thus the resulting expression for the field in the radiation zone entails a surface integral such as that which would arise if the source were two dimensional, i.e., if the source were concentrated into an infinitely thin sheet that coincided with the intersection of the coalescing sheets of the bifurcation surface with the source distribution.

For a two-dimensional source of this type, whether it be real or a virtual one whose field is described by a surface integral, the near zone (the Fresnel regime) of the radiation can extend to infinity, so that the amplitudes of the emitted waves are not necessarily subject to the spherical spreading that normally occurs in the far zone (the Fraunhofer regime). The Fresnel distance that marks the boundary between these two zones is given by $R_F \sim L_\perp^2/L_\parallel$, in which $L_\perp$ and $L_\parallel$ are the dimensions of the source perpendicular and parallel to the radiation direction. If the source is distributed over a surface and so has a dimension $L_\parallel$ that is vanishingly small, therefore, the Fresnel distance R_F tends to infinity.

In the present case the surface integral that arises from the discontinuity in the radiation effectiveness of the source elements across the bifurcation surface has an integrand that is in turn singular on the cusp curve of this surface. This has to do with the fact that the source elements on the cusp curve of the bifurcation surface approach the observer along the radiation direction not only with the wave speed but also with zero acceleration. The ratio of the emission to reception time intervals for the signals generated by these elements is by several orders of magnitude greater even than that for the elements on the bifurcation surface (see Appendix C). When the contributions of these elements are included in the surface integral in question, i.e., when the observation point is such that the cusp curve of the bifurcation surface intersects the source distribution (as shown in Fig. 6), the value of the resulting improper integral turns out to have the dependence $R_P^{-1/2}$, rather than R_P^{-1}, on the distance R_P of the observer from the source.

This nonspherically decaying component of the radiation is in addition to the conventional component that is concurrently generated by the remaining volume elements of the source. It is detectable only at those observation points, the cusp curves of whose bifurcation surfaces intersect the source distribution. It appears, therefore, as a spiral-shaped wave packet with the same azimuthal width as the $\hat{\varphi}$ extent of the source. For a source distribution whose superluminal portion extends from $\hat{r}=1$ to $\hat{r}_> > 1$, this wave packet is detectable, by an observer at infinity, within the angles $\frac{1}{2}\pi - \arccos \hat{r}_>^{-1} \leqslant \theta_P \leqslant \frac{1}{2}\pi + \arccos \hat{r}_>^{-1}$ from the rotation axis: Projection (12b) of the cusp curve of the bifurcation surface onto the (r,z) plane reduces to $\cot \theta_P = (\hat{r}^2-1)^{1/2}$ in the limit $R_P \to \infty$, where $\theta_P \equiv \arctan(r_P/z_P)$ [also see Eq. (54)].

Because it comprises a collection of the spiraling cusps of the envelopes of the wave fronts that are emitted by various source elements, this wave packet has a cross section with the plane of rotation whose extent and shape match those of the source distribution. It is a diffraction-free propagating caustic that, when detected by a far-field observer, would appear as a pulse of duration $\Delta\hat{\varphi}/\omega$, where $\Delta\hat{\varphi}$ is the azimuthal extent of the source.

Note that the waves that interfere constructively to form each cusp, and hence the observed pulse, are different at different observation times: The constituent waves propagate in the radiation direction $\hat{\mathbf{n}}$ with the speed c, whereas the propagating caustic that is observed, i.e., the segment of the cusp curve that passes through the observation point at the observation time, propagates in the azimuthal direction $\hat{\mathbf{e}}_{\varphi_P}$ with the phase speed $r_P\omega$.

The fact that the intensity of the pulse decays more slowly than predicted by the inverse square law is not therefore incompatible with the conservation of energy, for it is not the same wave packet that is observed at different distances from the source: The wave packet in question is constantly dispersed and reconstructed out of other waves. The cusp curve of the envelope of the wave fronts emanating from an infinitely long-lived source is detectable in the radiation zone not because any segment of this curve can be identified with a caustic that has formed at the source and has subsequently traveled as an isolated wave packet to the radiation zone, but because certain set of waves superpose coherently only at infinity.

The relative phases of the set of waves that are emitted during a limited time interval is such that these waves do not, in general, interfere constructively to form a cusped envelope until they have propagated some distance away from the source. The period in which this set of waves has a cusped envelope and so is detectable as a periodic train of nonspherically decaying pulses would of course have a limited duration if the source is short lived (cf. Appendix D). Thus pulses of focused waves may be generated by the present emission process that not only are stronger in the far field than any previously studied class of signals, but can in addition be beamed at only a select set of observers for a limited interval of time.

It should not be difficult to generate such pulses in the laboratory. The volume-distributed polarization current produced by applying a time-varying transverse electric field, or shining a radial beam of high-frequency ionizing radiation, around the circumference of a torus-shaped dielectric substance of radius ~ 1 m, for example, would in principle act as the required source of this new type of emission provided only the changes in the distribution of the resulting polarization current have a fixed pattern and propagate around the

torus with a constant angular frequency of the order of 10^8 rad/s.

A final remark is in order: The mechanism responsible for the effect described here is fundamentally different from that which gives rise to the Čerenkov effect. Because the presence of a cusp in the bifurcation surface (or in the envelope of the wave fronts emitted by a source point) is essential to this emission mechanism, the present effect does not come into play in the case of a rectilinearly moving source unless the motion of the source is accelerated. It has been shown in Appendix D, on the other hand, that in the superluminal regime the radiation generated by an accelerated rectilinearly moving source remains different from that generated by a corresponding constant-velocity source even in the limit in which the acceleration of the source tends to zero: In this limit, the cusp curve of the envelope merely moves to larger distances from the source rather than disappear.

ACKNOWLEDGMENTS

I thank J. E. Ffowcs Williams, J. H. Hannay, A. Hewish, and D. Lynden-Bell for extended discussions.

APPENDIX A: ASYMPTOTIC EXPANSIONS OF THE GREEN'S FUNCTIONS

In this appendix we calculate the leading terms in the asymptotic expansions of the integrals (16), (34), (42), and (52) for small $\phi_+ - \phi_-$, i.e., for points close to the cusp curve (12) of the bifurcation surface (or of the envelope of the wave fronts). The method, due to Chester, Friedman, and Ursell [13], that we use is a standard one that has been specifically developed for the evaluation of radiation integrals involving caustics (see [14] and [15]). The integrals evaluated below all have a phase function $g(\varphi)$ whose extrema ($\varphi = \varphi_\pm$) coalesce at the caustic (12).

As long as the observation point does not coincide with the source point, the function $g(\varphi)$ is analytic and the following transformation of the integration variables in Eq. (16) is permissible:

$$g(\varphi) = \tfrac{1}{3}\nu^3 - c_1^2\nu + c_2, \tag{A1}$$

where ν is the new variable of integration and the coefficients

$$c_1 \equiv (\tfrac{3}{4})^{1/3}(\phi_+ - \phi_-)^{1/3}, \quad c_2 \equiv \tfrac{1}{2}(\phi_+ + \phi_-) \tag{A2}$$

are chosen such that the values of the two functions on opposite sides of Eq. (A1) coincide at their extrema. Thus an alternative exact expression for G_0 is

$$G_0 = \int_{-\infty}^{+\infty} d\nu\, f_0(\nu)\, \delta(\tfrac{1}{3}\nu^3 - c_1^2\nu + c_2 - \phi), \tag{A3}$$

in which

$$f_0(\nu) \equiv R^{-1} d\varphi/d\nu. \tag{A4}$$

Close to the cusp curve (12), at which c_1 vanishes and the extrema $\nu = \pm c_1$ of the above cubic function are coincident, $f_0(\nu)$ may be approximated by $p_0 + q_0\nu$, with

$$p_0 = \tfrac{1}{2}(f_0|_{\nu=c_1} + f_0|_{\nu=-c_1}) \tag{A5}$$

and

$$q_0 = \tfrac{1}{2}c_1^{-1}(f_0|_{\nu=c_1} - f_0|_{\nu=-c_1}). \tag{A6}$$

The resulting expression

$$G_0 \sim \int_{-\infty}^{+\infty} d\nu (p_0 + q_0\nu)\, \delta(\tfrac{1}{3}\nu^3 - c_1^2\nu + c_2 - \phi) \tag{A7}$$

will then constitute, according to the general theory described in [13–15], the leading term in the asymptotic expansion of G_0 for small c_1 (see [17]).

To evaluate the integral in Eq. (A7) we need to know the roots of the cubic equation that follows from the vanishing of the argument of the Dirac δ function in this expression. Depending on whether the observation point is located inside or outside the bifurcation surface (the envelope), the roots of

$$\tfrac{1}{3}\nu^3 - c_1^2\nu + c_2 - \phi = 0 \tag{A8}$$

are given by

$$\nu = 2c_1 \cos(\tfrac{2}{3}n\pi + \tfrac{1}{3}\arccos\chi), \quad |\chi| < 1, \tag{A9a}$$

for $n = 0$, 1, and 2 or by

$$\nu = 2c_1 \operatorname{sgn}(\chi) \cosh(\tfrac{1}{3}\operatorname{arccosh}|\chi|), \quad |\chi| > 1, \tag{A9b}$$

respectively, where

$$\chi \equiv \left[\phi - \frac{1}{2}(\phi_+ + \phi_-)\right] \Big/ \left[\frac{1}{2}(\phi_+ - \phi_-)\right] = \frac{3}{2}(\phi - c_2)/c_1^3. \tag{A10}$$

Note that χ equals $+1$ on the sheet $\phi = \phi_+$ of the bifurcation surface (the envelope) and -1 on $\phi = \phi_-$.

The integral in Eq. (A7), therefore, has the following value when the observation point lies inside the bifurcation surface (the envelope):

$$\int_{-\infty}^{+\infty} d\nu\ \delta(\tfrac{1}{3}\nu^3 - c_1^2\nu + c_2 - \phi)$$

$$= \sum_{n=0}^{2} c_1^{-2} |4\cos^2(\tfrac{2}{3}n\pi + \tfrac{1}{3}\arccos\chi) - 1|^{-1}, \quad |\chi| < 1. \tag{A11}$$

Using the trignometric identity $4\cos^2\alpha - 1 = \sin 3\alpha/\sin\alpha$, we can write this as

$$\int_{-\infty}^{+\infty} d\nu\ \delta(\tfrac{1}{3}\nu^3 - c_1^2\nu + c_2 - \phi)$$

$$= c_1^{-2}(1-\chi^2)^{-1/2} \sum_{n=0}^{2} |\sin(\tfrac{2}{3}n\pi + \tfrac{1}{3}\arccos\chi)|$$

$$= 2c_1^{-2}(1-\chi^2)^{-1/2} \cos(\tfrac{1}{3}\arcsin\chi), \quad |\chi| < 1, \tag{A12}$$

in which we have evaluated the sum by adding the sine functions two at a time.

When the observation point lies outside the bifurcation surface (the envelope), the above integral receives a contribution only from the single value of ν given in Eq. (A9b) and we obtain

$$\int_{-\infty}^{+\infty} d\nu\ \delta(\tfrac{1}{3}\nu^3-c_1^2\nu+c_2-\phi) = c_1^{-2}(\chi^2-1)^{-1/2}\ \sinh(\tfrac{1}{3}\ \mathrm{arccosh}|\chi|), \quad |\chi|>1, \quad \text{(A13)}$$

where this time we have used the identity $4\cosh^2\alpha-1=\sinh 3\alpha/\sinh\alpha$. The second part of the integral in Eq. (A7) can be evaluated in exactly the same way. It has the value

$$\int_{-\infty}^{+\infty} d\nu\ \nu\ \delta(\tfrac{1}{3}\nu^3-c_1^2\nu+c_2-\phi) = 2c_1^{-1}(1-\chi^2)^{-1/2}\sum_{n=0}^{2}|\sin(\tfrac{2}{3}n\pi+\tfrac{1}{3}\ \arccos\chi)| \times\cos(\tfrac{2}{3}n\pi+\tfrac{1}{3}\ \arccos\chi) = -2c_1^{-1}(1-\chi^2)^{-1/2}\sin(\tfrac{2}{3}\ \arcsin\chi), \quad |\chi|<1, \quad \text{(A14)}$$

when the observation point lies inside the bifurcation surface (the envelope) and the value

$$\int_{-\infty}^{+\infty} d\nu\ \nu\ \delta(\tfrac{1}{3}\nu^3-c_1^2\nu+c_2-\phi) = c_1^{-1}(\chi^2-1)^{-1/2}\mathrm{sgn}(\chi)\sinh(\tfrac{2}{3}\ \mathrm{arccosh}|\chi|), \quad |\chi|>1, \quad \text{(A15)}$$

when the observation point lies outside the bifurcation surface (the envelope). Inserting Eqs. (A12)–(A15) in Eq. (A7) and denoting the values of G_0 inside and outside the bifurcation surface (the envelope) by G_0^{in} and G_0^{out}, we obtain

$$G_0^{\mathrm{in}}\sim 2c_1^{-2}(1-\chi^2)^{-1/2}[p_0\cos(\tfrac{1}{3}\ \arcsin\chi) - c_1 q_0\sin(\tfrac{2}{3}\ \arcsin\chi)], \quad |\chi|<1, \quad \text{(A16)}$$

and

$$G_0^{\mathrm{out}}\sim c_1^{-2}(\chi^2-1)^{-1/2}[p_0\sinh(\tfrac{1}{3}\ \mathrm{arccosh}|\chi|) + c_1 q_0\mathrm{sgn}(\chi)\sinh(\tfrac{2}{3}\ \mathrm{arccosh}|\chi|)], \quad |\chi|>1, \quad \text{(A17)}$$

for the leading terms in the asymptotic approximation to G_0 for small c_1.

The function $f_0(\nu)$ in terms of which the coefficients p_0 and q_0 are defined is indeterminate at $\nu=c_1$ and $-c_1$: Differentiation of Eq. (A1) yields $d\varphi/d\nu=(\nu^2-c_1^2)/(\partial g/\partial\varphi)$, the zeros of whose denominator at $\varphi=\varphi_-$ and φ_+, respectively, coincide with those of its numerator at $\nu=c_1$ and $-c_1$. This indeterminacy can be removed by means of l'Hôpital's rule by noting that

$$\left.\frac{d\varphi}{d\nu}\right|_{\nu=\pm c_1}=\left.\frac{\nu^2-c_1^2}{\partial g/\partial\varphi}\right|_{\nu=\pm c_1}=\left.\frac{2\nu}{(\partial^2 g/\partial\varphi^2)(d\varphi/d\nu)}\right|_{\nu=\pm c_1}, \quad \text{(A18)}$$

i.e., that

$$\left.\frac{d\varphi}{d\nu}\right|_{\nu=\pm c_1}=\left.\left(\frac{\pm 2c_1}{\partial^2 g/\partial\varphi^2}\right)^{1/2}\right|_{\varphi=\varphi_\mp}=\frac{(2c_1\hat{R}_\mp)^{1/2}}{\Delta^{1/4}}, \quad \text{(A19)}$$

in which we have calculated $(\partial^2 g/\partial\varphi^2)_{\varphi_\pm}$ from Eqs. (7) and (8). The right-hand side of Eq. (A19) is in turn indeterminate on the cusp curve of the bifurcation surface (the envelope) where $c_1=\Delta=0$. Removing this indeterminacy by expanding the numerator in this expression in powers of $\Delta^{1/4}$, we find that $d\varphi/d\nu$ assumes the value $2^{1/3}$ at the cusp curve.

Hence the coefficients p_0 and q_0 that appear in the expressions (A16) and (A17) for G_0 are explicitly given by

$$p_0=(\omega/c)(\tfrac{1}{2}c_1)^{1/2}(\hat{R}_-^{-1/2}+\hat{R}_+^{-1/2})\Delta^{-1/4} \quad \text{(A20)}$$

and

$$q_0=(\omega/c)(2c_1)^{-1/2}(\hat{R}_-^{-1/2}-\hat{R}_+^{-1/2})\Delta^{-1/4} \quad \text{(A21)}$$

[see Eqs.(A4)–(A6) and (A19)]. In the regime of validity of Eqs. (A16) and (A17), where Δ is much smaller than $(\hat{r}_P^2\hat{r}^2-1)^{1/2}$, the leading terms in the expressions for $\hat{R}_\pm$, c_1, p_0, and q_0 are

$$\hat{R}_\pm=(\hat{r}_P^2\hat{r}^2-1)^{1/2}\pm(\hat{r}_P^2\hat{r}^2-1)^{-1/2}\Delta^{1/2}+O(\Delta), \quad \text{(A22)}$$

$$c_1=2^{-1/3}(r_P^2\hat{r}^2-1)^{-1/2}\Delta^{1/2}+O(\Delta), \quad \text{(A23)}$$

$$p_0=2^{1/3}(\omega/c)(\hat{r}^2\hat{r}_P^2-1)^{-1/2}+O(\Delta^{1/2}), \quad \text{(A24)}$$

and

$$q_0=2^{-1/3}(\omega/c)(\hat{r}^2\hat{r}_P^2-1)^{-1}+O(\Delta^{1/2}). \quad \text{(A25)}$$

These may be obtained by using Eq. (9) to express $\hat{z}$ everywhere in Eqs. (10), (11), and (A2) in terms of Δ and $\hat{r}$ and expanding the resulting expressions in powers of $\Delta^{1/2}$. The quantity Δ in turn has the following value at points $0\leqslant\hat{z}_c-\hat{z}\ll(\hat{r}_P^2-1)^{1/2}(\hat{r}^2-1)^{1/2}$:

$$\Delta=2(\hat{r}_P^2-1)^{1/2}(\hat{r}^2-1)^{1/2}(\hat{z}_c-\hat{z})+O[(\hat{z}_c-\hat{z})^2], \quad \text{(A26)}$$

in which $\hat{z}_c$ is given by the expression with the plus sign in Eq. (12b). For an observation point in the far zone ($\hat{r}_P\gg 1$), the above expressions reduce to

$$\hat{R}_\pm\sim\hat{r}\hat{r}_P, \quad c_1\simeq 2^{1/6}(\hat{r}\hat{r}_P)^{-1/2}(1-\hat{r}^{-2})^{1/4}(\hat{z}_c-\hat{z})^{1/2}; \quad \text{(A27)}$$

$$\Delta\simeq 2\hat{r}_P(\hat{r}^2-1)^{1/2}(\hat{z}_c-\hat{z}); \quad \text{(A28)}$$

$$p_0\simeq 2^{1/3}(\omega/c)(\hat{r}_P\hat{r})^{-1}, \quad q_0\simeq 2^{-1/3}(\omega/c)(\hat{r}_P\hat{r})^{-2}, \quad \text{(A29)}$$

and

$$\chi \simeq 3(\tfrac{1}{2}\hat{r}\hat{r}_P)^{3/2}(1-\hat{r}^{-2})^{-3/4}(\phi-\phi_c)/(\hat{z}_c-\hat{z})^{3/2}, \tag{A30}$$

in which $\hat{z}_c-\hat{z}$ has been assumed to be finite.

Evaluation of the other Green's functions $\mathbf{G}_1$, $\mathbf{G}_2$, and $\mathbf{G}_3$ entails calculations that have many steps in common with that of G_0. Since the integrals in Eqs. (34), (42), and (52) differ from that in Eq. (16) only in that their integrands respectively contain the extra factors $\hat{\mathbf{n}}$, $\hat{\mathbf{e}}_\varphi$, and $\hat{\mathbf{n}}\times\hat{\mathbf{e}}_\varphi$, they can be rewritten as integrals of the form (A3) in which the functions

$$\mathbf{f}_1(\nu)\equiv\hat{\mathbf{n}}f_0, \quad \mathbf{f}_2(\nu)\equiv\hat{\mathbf{e}}_\varphi f_0, \quad \mathbf{f}_3(\nu)\equiv\hat{\mathbf{n}}\times\hat{\mathbf{e}}_\varphi f_0 \tag{A31}$$

replace the $f_0(\nu)$ given by Eq. (A4).

If p_0 and q_0 are correspondingly replaced, in accordance with Eqs. (A5) and (A6), by

$$\mathbf{p}_k=\tfrac{1}{2}(\mathbf{f}_k|_{\nu=c_1}+\mathbf{f}_k|_{\nu=-c_1}), \quad k=1,2,3, \tag{A32}$$

and

$$\mathbf{q}_k=\tfrac{1}{2}c_1^{-1}(\mathbf{f}_k|_{\nu=c_1}-\mathbf{f}_k|_{\nu=-c_1}), \quad k=1,2,3, \tag{A33}$$

then every step of the analysis that led from Eq. (A7) to Eqs. (A16) and (A17) would be equally applicable to the evaluation of $\mathbf{G}_k$. It follows, therefore, that

$$\mathbf{G}_k^{\rm in}\sim 2c_1^{-2}(1-\chi^2)^{-1/2}[\mathbf{p}_k\cos(\tfrac{1}{3}\arcsin\chi) - c_1\mathbf{q}_k\sin(\tfrac{2}{3}\arcsin\chi)], \quad |\chi|<1, \tag{A34}$$

and

$$\mathbf{G}_k^{\rm out}\sim c_1^{-2}(\chi^2-1)^{-1/2}[\mathbf{p}_k\sinh(\tfrac{1}{3}\,\mathrm{arccosh}|\chi|) + c_1\mathbf{q}_k\,\mathrm{sgn}(\chi)\sinh(\tfrac{2}{3}\,\mathrm{arccosh}|\chi|)], \quad |\chi|>1, \tag{A35}$$

constitute the uniform asymptotic approximations to the functions $\mathbf{G}_k$ inside and outside the bifurcation surface (the envelope) $|\chi|=1$.

Explicit expressions for $\mathbf{p}_k$ and $\mathbf{q}_k$ as functions of (r,z) may be found from Eqs. (8), (A19), and (A31)–(A33) jointly. The result is

$$\left.\begin{matrix}\mathbf{p}_1\\ \mathbf{q}_1\end{matrix}\right\} = 2^{-1/2}(\omega/c)c_1^{\pm 1/2}\Delta^{-1/4}\{[(\hat{r}_P-\hat{r}_P^{-1})(\hat{R}_-^{-3/2}\pm\hat{R}_+^{-3/2}) - \hat{r}_P^{-1}\Delta^{1/2}(\hat{R}_-^{-3/2}\mp\hat{R}_+^{-3/2})]\hat{\mathbf{e}}_{r_P} + \hat{r}_P^{-1}(\hat{R}_-^{-1/2}\pm\hat{R}_+^{-1/2})\hat{\mathbf{e}}_{\varphi_P} + (\hat{z}_P-\hat{z})(\hat{R}_-^{-3/2}\pm\hat{R}_+^{-3/2})\hat{\mathbf{e}}_{z_P}\}, \tag{A36}$$

$$\left.\begin{matrix}\mathbf{p}_2\\ \mathbf{q}_2\end{matrix}\right\} = 2^{-1/2}(\omega/c)(\hat{r}\hat{r}_P)^{-1}c_1^{\pm 1/2}\Delta^{-1/4}\{(\hat{R}_-^{1/2}\pm\hat{R}_+^{1/2})\hat{\mathbf{e}}_{r_P} + [\hat{R}_-^{-1/2}\pm\hat{R}_+^{-1/2}+\Delta^{1/2}(\hat{R}_-^{-1/2}\mp\hat{R}_+^{-1/2})]\hat{\mathbf{e}}_{\varphi_P}\}, \tag{A37}$$

and

$$\left.\begin{matrix}\mathbf{p}_3\\ \mathbf{q}_3\end{matrix}\right\} = 2^{-1/2}(\omega/c)(\hat{r}\hat{r}_P)^{-1}c_1^{\pm 1/2}\Delta^{-1/4}\{-(\hat{z}_P-\hat{z}) \times[\hat{R}_-^{-3/2}\pm\hat{R}_+^{-3/2}+\Delta^{1/2}(\hat{R}_-^{-3/2}\mp\hat{R}_+^{-3/2})]\hat{\mathbf{e}}_{r_P} + (\hat{z}_P-\hat{z})(\hat{R}_-^{-1/2}\pm\hat{R}_+^{-1/2})\hat{\mathbf{e}}_{\varphi_P} + \hat{r}_P[\Delta^{1/2}(\hat{R}_-^{-3/2}\mp\hat{R}_+^{-3/2}) - (\hat{r}^2-1)(\hat{R}_-^{-3/2}\pm\hat{R}_+^{-3/2})]\hat{\mathbf{e}}_{z_P}\}, \tag{A38}$$

where use has been made of the fact that $\hat{\mathbf{e}}_\varphi=-\sin(\varphi-\varphi_P)\hat{\mathbf{e}}_{r_P}+\cos(\varphi-\varphi_P)\hat{\mathbf{e}}_{\varphi_P}$. Here the expressions with the upper signs yield the $\mathbf{p}_k$ and those with the lower signs the $\mathbf{q}_k$.

The asymptotic value of each $\mathbf{G}_k^{\rm out}$ is indeterminate on the bifurcation surface (the envelope). If we expand the numerator of Eq. (A35) in powers of its denominator and cancel out the common factor $(\chi^2-1)^{1/2}$ prior to evaluating the ratio in this equation, we obtain

$$\mathbf{G}_k^{\rm out}|_{\phi=\phi_\pm}=\mathbf{G}_k^{\rm out}|_{\chi=\pm 1}\sim(\mathbf{p}_k\pm 2c_1\mathbf{q}_k)/(3c_1^2). \tag{A39}$$

This shows that $\mathbf{G}_k^{\rm out}|_{\phi=\phi_-}$ and $\mathbf{G}_k^{\rm out}|_{\phi=\phi_+}$ remain different even in the limit where the surfaces $\phi=\phi_-$ and ϕ_+ coalesce. The coefficients $\mathbf{q}_k$ that specify the strengths of the discontinuities

$$\mathbf{G}_k^{\rm out}|_{\phi=\phi_+}-\mathbf{G}_k^{\rm out}|_{\phi=\phi_-}\sim\tfrac{4}{3}\mathbf{q}_k/c_1 \tag{A40}$$

reduce to

$$\mathbf{q}_1\simeq\frac{3}{2^{1/3}}(\omega/c)(\hat{r}\hat{r}_P)^{-3}[(1-\tfrac{2}{3}\hat{r}^2)\hat{r}_P\hat{\mathbf{e}}_{r_P}+(\hat{z}_P-\hat{z})\hat{\mathbf{e}}_{z_P}], \tag{A41}$$

$$\mathbf{q}_2\simeq 2^{2/3}(\omega/c)(\hat{r}\hat{r}_P)^{-1}\hat{\mathbf{e}}_{\varphi_P}, \tag{A42}$$

and

$$\mathbf{q}_3\simeq-2^{2/3}(\omega/c)(\hat{r}\hat{r}_P)^{-2}[(\hat{z}_P-\hat{z})\hat{\mathbf{e}}_{r_P}-\hat{r}_P\hat{\mathbf{e}}_{z_P}] \tag{A43}$$

in the regime of validity of Eqs. (A27) and (A28). When $0\leqslant\hat{z}_c-\hat{z}\ll(\hat{r}^2-1)^{1/2}\hat{r}_P$, the expressions (A41) and (A43) further reduce to

$$\mathbf{q}_1\simeq\frac{3}{2^{1/3}}(\omega/c)(\hat{r}\hat{r}_P)^{-2}\mathbf{n}_1, \quad \mathbf{q}_3\simeq 2^{2/3}(\omega/c)(\hat{r}\hat{r}_P)^{-1}\mathbf{n}_3, \tag{A44}$$

with

$$\mathbf{n}_1\equiv(\hat{r}^{-1}-\tfrac{2}{3}\hat{r})\hat{\mathbf{e}}_{r_P}-(1-\hat{r}^{-2})^{1/2}\hat{\mathbf{e}}_{z_P}, \quad \mathbf{n}_3\equiv(1-\hat{r}^{-2})^{1/2}\hat{\mathbf{e}}_{r_P}+\hat{r}^{-1}\hat{\mathbf{e}}_{z_P}, \tag{A45}$$

for in this case Eq. (12b), with the adopted plus sign, can be used to replace $\hat{z}-\hat{z}_P$ by $(\hat{r}^2-1)^{1/2}\hat{r}_P$.

APPENDIX B: ALTERNATIVE FORMS OF THE RADIATION INTEGRALS

In this paper we have built up the potential of an extended source distribution by superposing the potentials of the moving source elements that constitute it. Stated mathematically,

we have expressed the potential (24) as the convolution of the source density with the Green's function for the problem. An alternative procedure is one in which the potential of the moving extended source is built up from the superposition of the potentials of a fictitious set of stationary point sources. This can be done by basing the analysis on the alternative form of the retarded potential given in Eq. (22). For fixed values of $(\mathbf{x}_P,\ t_P)$, the expression in Eq. (22) is the same as that which would describe the potential of a time-independent source with the density distribution $\rho(\mathbf{x}, t_P - |\mathbf{x} - \mathbf{x}_P|/c)$.

The alternative form of the scalar potential that follows from Eqs. (22) and (23) has an integrand that is singularity free in the radiation zone:

$$A_0(r_P,\hat{\varphi}_P,z_P)=\int r\ dr\ dz\ d\varphi\ \rho(r,z,\hat{\varphi}|_{t=t_P-R/c})/R, \tag{B1}$$

where R is the function defined in Eq. (3). It may at first seem, therefore, that the bifurcation surface, which featured so prominently in our calculation of $\nabla_P A_0$, for instance, neither appears nor plays any role in the present formulation of the problem. Our objective in this appendix is to point out that this is not so: An analysis based on Eq. (B1) also entails a handling of the singularities that occur on the bifurcation surface and ultimately results in the same value for $\nabla_P A_0$.

The given data in the present problem consist of the source density ρ as a function of $(r,\hat{\varphi},z)$ and the Sommerfeld radiation condition at infinity. The boundary of the source distribution is known in the $(r,\hat{\varphi},z)$ space and not in the (r,φ,z) space over which the integration in Eq. (B1) is to be performed. In the (r,φ,z) space, the surface at which $\rho(r,z,\hat{\varphi}|_{t=t_P-R/c})$ vanishes is different for different observers, or at different observation times, and is a multiple-sheeted disconnected surface whose shape bears no direct relationship with the shape of the actual source distribution. To find the limits of integration in Eq. (B1), we need to use the relationship

$$\hat{\varphi}=(\varphi-\omega t)|_{t=t_P-R/c}=\varphi-\omega t_P+[(\hat{z}-\hat{z}_P)^2+\hat{r}^2+\hat{r}_P^2 - \hat{r}\hat{r}_P\cos(\varphi-\varphi_P)]^{1/2} \tag{B2}$$

between φ and the retarded value of $\hat{\varphi}$ that appears in the argument of ρ to map the boundaries $\hat{\varphi}=\hat{\varphi}_<(r,z)$ and $\hat{\varphi}=\hat{\varphi}_>(r,z)$ of the source distribution from the $(r,\hat{\varphi},z)$ space to the (r,φ,z) space.

Figure 2 depicts the relation (B2), in its alternative form (5), for fixed values of $(r_P,\hat{\varphi}_P,z_P;r,z)$. Two adjacent extrema of curve (a) in Fig. 2 occur on two different sheets of the bifurcation surface: The constant values (r_0,z_0) of (r,z) in this figure are such that the circle $r=r_0,\ z=z_0$ intersects the bifurcation surface, so that as $\hat{\varphi}$ ranges over the interval shown in the figure the point $(r,\hat{\varphi},z)$ enters across one sheet, traverses the interior, and leaves across another sheet of the bifurcation surface. At those points on the source boundary that lie within the bifurcation surface, therefore, the required mapping $\hat{\varphi}\to\varphi$ of the limits of integration in Eq. (B1) is multivalued.

The limits of the integration with respect to φ in Eq. (B1) are given by the solutions $\varphi(r,\hat{\varphi},z;r_P,\hat{\varphi}_P,z_P;\varphi_P)$ of Eq. (B2) or (5) for a point $(r,\hat{\varphi},z)$ on the boundary of the source distribution. Differentiating Eq. (5) with respect to $\mathbf{x}_P$ while holding $(r,\hat{\varphi},z)$ and the observation time $\hat{\varphi}_P$ constant, we find that the derivatives of these integration limits are given by an expression

$$\nabla_P\varphi=r_P^{-1}\hat{\mathbf{e}}_{\varphi_P}-\{[\hat{r}_P-\hat{r}\ \cos(\varphi-\varphi_P)]\hat{\mathbf{e}}_{r_P} + (\hat{z}_P-\hat{z})\hat{\mathbf{e}}_{z_P}\}/(R\partial g/\partial\varphi) \tag{B3}$$

whose denominator vanishes on the bifurcation surface. In fact, this expression has an even stronger singularity on the cusp curve of the bifurcation surface at which its denominator both vanishes and has a vanishing derivative.

Whenever the boundary of the source distribution intersects the bifurcation surface or its cusp curve, therefore, the integral in Eq. (B1) is not differentiable (as a classical function) because the contributions from the derivatives of its limits to the value of $\nabla_P A_0$ would appear as a two-dimensional integral whose integrand has extended singularities. If we denote the upper and lower limits of the integration with respect to φ by $\varphi_>$ and $\varphi_<$ and the projection of the source distribution onto the (r,z) plane by S_{rz}, then the contributions in question would appear as

$$\int_{S_{rz}} r\ dr\ dz\{[\rho/R]_{\varphi=\varphi_>}\nabla_P\varphi_>-[\rho/R]_{\varphi=\varphi_<}\nabla_P\varphi_<\}, \tag{B4}$$

in which $\nabla_P\varphi_>$ and $\nabla_P\varphi_<$ are given by Eq. (B3) and so diverge at the points $\varphi=\varphi_\pm$ on the intersection of the boundary of the source with the bifurcation surface. That is to say, contrary to what may seem at first, the calculation of $\nabla_P A_0$ from Eq. (B1) likewise requires a proper handling (with the aid, e.g., of the theory of generalized functions) of the extended singularities that occur on the bifurcation surface and its cusp curve.

Hannay [18] has argued that since the only singularity of the integrand of Eq. (22) is that at the point $\mathbf{x}=\mathbf{x}_P$, which is inoffensive, one can differentiate Eq. (22) under the integral sign and evaluate the resulting expressions for $\nabla_P A_0$ and $\partial A_0/\partial t_P$ without any reference to the bifurcation surface. Being based on an analysis in which neither the motion of the source nor the position of the observer are specified, however, Hannay's argument overlooks the specifically superluminal feature of the problem that appears in Eq. (B3): Whereas, in the familiar subluminal regime, the contributions to $\nabla_P A_0$ or $\partial A_0/\partial t_P$ from the derivatives of the limits of the φ integration in Eq. (B1) are either zero or cancel each other, here the corresponding contributions of those elements on the boundary of the source that approach the observer with the wave speed are divergent. Leibniz's formula for the differentiation of a definite integral (as a classical function) is not of course applicable if there are any points at which the contributions from the limits of integration diverge.

APPENDIX C: RATIO OF EMISSION TO RECEPTION TIME INTERVALS

The interval of retarded time δt during which a set of waves are emitted is, in the case of the source elements that lie adjacent to but inside the bifurcation surface, significantly longer than the interval of observation time δt_P during which these waves are received. The components of the velocities of such elements in the direction $\mathbf{x}_P-\mathbf{x}$ are either just above or just below the wave speed at the two coalescing retarded times at which these elements make their dominant contributions, so that, as in the Doppler effect, the emitted wave fronts pile up along this radiation direction.

In this appendix we estimate the ratio of emission to reception time intervals for three sets of source elements: the elements in the vicinity of the cusp curve of the bifurcation surface and the elements adjacent to the bifurcation surface, just inside and just outside it. These three sets of elements respectively approach the observer along the radiation direction with the wave speed and zero acceleration, with the wave speed and a nonzero acceleration, and with a speed different from c and an acceleration different from zero.

Given the observation point (r_P,φ_P,z_P) and the moving source point $(r,\hat{\varphi},z)$, the equation describing the wave fronts [i.e., Eq. (4)] specifies the reception time t_P as the following function of the emission time t:

$$t_P=t+[(z_P-z)^2+r_P^2+r^2-2r_Pr\,\cos(\varphi_P-\hat{\varphi}-\omega t)]^{1/2}/c. \tag{C1}$$

Calculating the first three derivatives of t_P with respect to t from Eq. (C1) and evaluating these derivatives at the cusp curve (12) of the bifurcation surface, we find that the dominant term in the Taylor expansion of t_P about the value t_c of the retarded time, at which an element on this curve makes its contribution, is given by

$$\delta t_P=\frac{1}{3!}\,d^3t_P/dt^3|_{t=t_c}(\delta t)^3+\cdots=\tfrac{1}{6}\omega^2(\delta t)^3+\cdots\,, \tag{C2}$$

where t_c is defined by $(\varphi_c-\hat{\varphi})/\omega$ with the φ_c given in Eq. (12c). That is to say, the ratio of emission to reception time intervals has the value $\delta t/\delta t_P\simeq 6^{1/3}(\omega\delta t_P)^{-2/3}$ for the waves that are generated by the source elements at the cusp curve.

To estimate the numerical value of this ratio, let us denote the wavelength of the radiation by λ and consider the set of wave fronts that arrive at the observer within the time interval $\delta t_P=\frac{1}{2}\lambda/c$, i.e., that are received with essentially the same phase. For this set of waves, the ratio in question has the value

$$\delta t/\delta t_P\simeq 2\times 3^{1/3}(\lambda\omega/c)^{-2/3}, \tag{C3}$$

a value that could exceed unity by a large factor: For $\lambda\sim 1$ cm and $\omega\sim 2\pi$ rad/s (as in the case of pulsars), this ratio is of the order of 10^7.

Approaching the sheet $\phi=\phi_+$ or ϕ_- of the bifurcation surface from inside this surface corresponds to raising or lowering a horizontal line $g=\phi_0=$const with $\phi_-\leqslant\phi_0\leqslant\phi_+$ in Fig. 2 until it intersects curve (a) of this figure at its maximum or minimum. At a source point thus approached, dt_P/dt vanishes but d^2t_P/dt^2 is nonzero, so that the Taylor expansions of Eq. (C1) about the values $t_\pm\equiv(\varphi_\pm-\hat{\varphi})/\omega$ of the retarded time on the two sheets of the bifurcation surface assume the forms

$$\delta t_P=\mp\,\omega(2\hat{r}\hat{r}_P)^{-1/2}(1-\hat{r}^{-2})^{1/4}(\hat{z}_c-\hat{z})^{1/2}(\delta t)^2+\cdots\,, \tag{C4}$$

in which we have approximated the coefficient of $(\delta t)^2$ by its value for $0\leqslant\hat{z}_c-\hat{z}\ll 1$, $\hat{r}_P\gg 1$ [see Eqs. (26), (A20), and (A21)].

For the waves that arrive at the observer with a phase difference $c\,\delta t_P/\lambda\leqslant\frac{1}{2}$, therefore, Eq. (C4) yields

$$\delta t/\delta t_P\simeq\mp\,2^{3/4}(\hat{r}\hat{r}_P)^{1/4}(1-\hat{r}^{-2})^{-1/8}(\hat{z}_c-\hat{z})^{-1/4}(\lambda\omega/c)^{-1/2}. \tag{C5}$$

With the values of ω and λ adopted above, this is $\sim 10^5$ for a source point on the bifurcation surface that lies at a distance $\hat{z}_c-\hat{z}$ of the order of $\hat{r}_P$ from the cusp curve. [Note that the quadratic term in Eq. (C4) dominates the cubic term in this series only at distances $\hat{z}_c-\hat{z}$ of the order of $\hat{r}_P$ from the cusp curve.]

On the other hand, for a neighboring source point that lies just outside the sheet $\phi=\phi_-$ (say) of the bifurcation surface, curve (a) in Fig. 2 will have the same shape but the line $g=\phi_0$ will be displaced such that it would lie just below the minimum of g. Thus the equation $g(\varphi)=\phi_-$ has only a single physically relevant solution $\varphi=\varphi_{\rm out}$ in this case, a solution that is different from $\varphi_\pm$ and so at which $\partial g/\partial\varphi$ does not vanish. The neighboring source point just inside the bifurcation surface of course makes a contribution at the retarded time corresponding to $\varphi=\varphi_{\rm out}$ as well as at the two retarded times that coalesce onto $t_-=(\varphi_--\hat{\varphi})/\omega$. However, the component of its speed along the radiation direction has the limiting value c only at the two retarded times that coalesce onto t_-. At the retarded time corresponding to $\varphi=\varphi_{\rm out}$, at which the slope of the curve representing $g(\varphi)$ is different from zero (see Fig. 2), neither of the two neighboring source points approach the observer with the wave speed.

We can find $\varphi_{\rm out}$ for a source point that lies adjacent to the sheet $\phi=\phi_-$ of the bifurcation surface, close to the cusp curve, by replacing $g(\varphi)$ with the first three terms in its Taylor expansion about $\varphi=\varphi_-$ and by noting that the solution, different from $\varphi=\varphi_-$, of the resulting cubic equation $g(\varphi)=\phi_-$ is given by

$$\varphi_{\rm out}\simeq\varphi_--3(\tfrac{1}{2}\hat{r}\hat{r}_P)^{-1/2}(1-\hat{r}^{-2})^{1/4}(\hat{z}_c-\hat{z})^{1/2} \tag{C6}$$

for $0\leqslant\hat{z}_c-\hat{z}\ll 1$ and $\hat{r}_P\gg 1$. Next expanding Eq. (C1) about the corresponding value $t_{\rm out}=(\hat{\varphi}-\varphi_{\rm out})/\omega$ of t and approximating the coefficient of the dominant term in the resulting Taylor series by its far-field value for $0\leqslant\hat{z}_c-\hat{z}\ll 1$, we obtain

$$\delta t_P=3(\hat{r}\hat{r}_P)^{-1}(1-\hat{r}^{-2})^{1/2}(\hat{z}_c-\hat{z})\,\delta t+\cdots\,. \tag{C7}$$

Hence there is no new effect in the case of a source element that lies adjacent to but outside the bifurcation surface: The emission time interval is proportional to the reception time interval as in conventional emission mechanisms.

Insofar as the ratio $\delta t/\delta t_P$ is a measure of the degree of coherence of the emission from a given source element, a comparison of Eqs. (C3) and (C7) suggests, therefore, that the radiation effectiveness of the source elements should undergo a discontinuity across the bifurcation surface. This suggestion, which has here emerged from a consideration of the propagation properties of the wave fronts, is in fact confirmed by the calculation (in Sec. III) of the amplitudes of the emitted waves from Maxwell's equations.

Hewish [19] has presented a geometrical argument whose central result is expression (C3) for the ratio $(\delta t/\delta t_P)_{\text{cusp}}$. He contends that the coherence factor implied by this ratio constitutes the only difference between the intensities of the emissions that would arise from the superluminal and subluminal portions of the rotating sources in pulsars. As we have seen, however, Eq. (C3) merely describes a single isolated feature of the complicated emission process under discussion. It is not until it is compared with Eqs. (C5) and (C7) that its full implications, those pointing to the discontinuity in the radiative effectiveness of the source elements across the bifurcation surface, emerge. Even then, these implications of an analysis that is based on geometrical optics can at best be suggestive. The effect of the implied discontinuity on the intensity of the radiation produced by such an unfamiliar mechanism as that involved here cannot be predicted without examining the relevant solution of the exact wave equation itself.

APPENDIX D: RECTILINEARLY MOVING ACCELERATED SOURCES WITH SUPERLUMINAL VELOCITIES

Though perhaps less interesting from a practical point of view, the rectilinear version of the emission process we have discussed above is simpler in its caustic geometry and so conceptually more transparent. Here we include an analysis of this more elementary problem to illustrate not only the basic principles common to different examples of the emission process under discussion but also those of its features that specifically arise from the finiteness of the duration of the source.

Consider a point source (an element of the propagating distribution pattern of a volume source) that moves parallel to the z axis of a Cartesian coordinate system with the constant acceleration a, i.e., whose path $\mathbf{x}(t)$ is given by

$$x=\text{const}, \quad y=\text{const}, \quad z=\tilde{z}+ut+\tfrac{1}{2}at^2, \tag{D1}$$

where $\tilde{z}$ and u are its position and its speed at the time $t=0$. The wave fronts that are emitted by this source in an empty and unbounded space are described by Eq. (2). Inserting Eq. (D1) in Eq. (2) and squaring the resulting equation, we obtain

$$\begin{aligned}\overline{R^2}(t)\equiv&(x_P-x)^2+(y_P-y)^2+(z_P-\tilde{z}-ut-\tfrac{1}{2}at^2)^2\\ &=c^2(t_P-t)^2,\end{aligned} \tag{D2}$$

in which the coordinates (x_P,y_P,z_P,t_P) mark the space-time of observation points. These wave fronts are expanding spheres of radii $c(t_P-t)$ whose fixed centers $(x_P=x,\ y_P=y,\ z_P=\tilde{z}+ut+\frac{1}{2}at^2)$ depend on their emission times t (see Fig. 7).

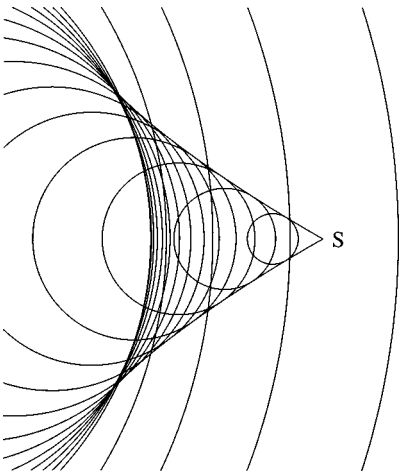

FIG. 7. Wave fronts emanating from the rectilinearly moving source point S and their envelope for $\beta_P=2$ (and $M<1$).

Introducing the natural length scale of the problem $l=c^2/a$, we can express Eq. (D2) in terms of dimensionless variables as

$$\begin{aligned}\overline{g}\equiv&\tfrac{1}{4}\beta^4-(\tfrac{1}{2}\beta_P^2-\zeta+1)\beta^2+2\beta_P\beta+(\tfrac{1}{2}\beta_P^2-\zeta)^2-\beta_P^2+\xi^2\\ &=0,\end{aligned} \tag{D3}$$

in which

$$\xi\equiv[(x-x_P)^2+(y-y_P)^2]^{1/2}/l \tag{D4}$$

represents the distance (in units of l) of the observation point from the path of the source, the Lagrangian coordinate

$$\zeta\equiv(\tilde{z}-\tilde{z}_P)/l \tag{D5}$$

stands for the difference between the positions $\tilde{z}=z-ut-\frac{1}{2}at^2$ of the source point and

$$\tilde{z}_P\equiv z_P-ut_P-\tfrac{1}{2}at_P^2 \tag{D6}$$

of the observation point in the $(x,y,\tilde{z})$ space, and the ''Mach numbers''

$$\beta\equiv(u+at)/c, \quad \beta_P\equiv(u+at_P)/c \tag{D7}$$

denote the scaled values of the emission time and the observation time, respectively. Figure 7 depicts the wave fronts described by Eq. (D3) for a fixed value of β_P and a discrete set of values of β $(<\beta_P)$.

The wave fronts for which $\beta>1$, i.e., the wave fronts that are emitted when the speed of the source exceeds the wave speed, possess an envelope: The function $\overline{g}(\beta)$ is oscillatory in this regime (see Fig. 8) and so there are points (ξ,ζ) at which

$$\partial\overline{g}/\partial\beta=\beta^3-(\beta_P^2-2\zeta+2)\beta+2\beta_P=0. \tag{D8}$$

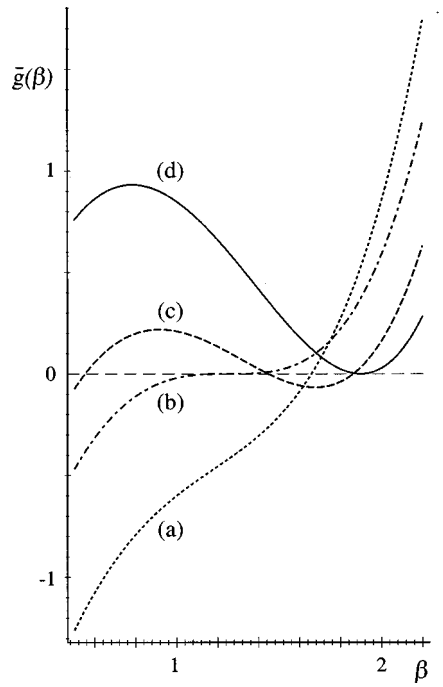

FIG. 8. Curve representing $\overline{g}(\beta)$ versus β for $\beta_P=2$, at a given (ξ, ζ): (*a*) at (0.2, 0.9) outside the envelope (or the bifurcation surface), (*b*) at (ξ_c, ζ_c) on the cusp curve of the envelope (or the bifurcation surface), (*c*) at (0, 0.4) inside the envelope (or the bifurcation surface), and (*d*) at (0.085, 0.142) on the envelope (or the bifurcation surface).

The cubic equation (D8) has three real roots when $3^{3/2}\beta_P(\beta_P^2-2\zeta+2)^{-3/2}<1$, of which only two satisfy the requirement $\beta>0$. These two physically relevant solutions of Eq. (D8) are

$$\beta_{\pm}=\frac{2}{\sqrt{3}}\,(\beta_P^2-2\zeta+2)^{1/2}\cos[\tfrac{1}{3}(\pi\pm\sigma)], \tag{D9a}$$

where

$$\sigma\equiv\arccos[3^{3/2}\beta_P(\beta_P^2-2\zeta+2)^{-3/2}]. \tag{D9b}$$

The function $\overline{g}(\beta)$ is locally maximum at β_+ and minimum at β_-.

Inserting $\beta=\beta_{\pm}$ in Eq. (D3) and solving the resulting equation for ξ as a function of ζ, we find that the envelope of the wave fronts is an axisymmetric surface consisting of two sheets: $\xi=\xi_{\pm}(\zeta)$ with

$$\xi_{\pm}\equiv[\tfrac{1}{2}(\tfrac{1}{2}\beta_P^2-\zeta+1)\beta_{\mp}^2-\tfrac{3}{2}\beta_P\beta_{\mp}+\beta_P^2-(\tfrac{1}{2}\beta_P^2-\zeta)^2]^{1/2}. \tag{D10}$$

[We have used the fact that $\beta_{\pm}$ satisfy Eq. (D8) to simplify the above expressions for $\xi_{\pm}$.]

The cusp of the envelope (see Fig. 7) occurs along the circle

$$\xi=(\beta_P^{2/3}-1)^{3/2}\equiv\xi_c, \quad \zeta=\tfrac{1}{2}\beta_P^2-\tfrac{3}{2}\beta_P^{2/3}+1\equiv\zeta_c. \tag{D11a}$$

When $\xi=\xi_c$, $\zeta=\zeta_c$, the function $\overline{g}(\beta)$, shown in Fig. 8, curve (*b*), has a point of inflection and $\partial^2\overline{g}/\partial\beta^2$, as well as $\partial\overline{g}/\partial\beta$ and $\overline{g}$, vanishes at

$$\beta=\beta_P^{1/3}\equiv\beta_c. \tag{D11b}$$

The cusp propagates with the speeds $(1-\beta_P^{-2/3})^{1/2}c$ and $\beta_P^{-1/3}c$ in the directions perpendicular and parallel to the source's path, respectively, so that the coincident sheets of the envelope at the cusp propagate normal to themselves, in a direction making the angle $\arctan(\beta_P^{2/3}-1)^{1/2}$ with the $\tilde{z}_P$ axis, at the speed c.

The tangential wave fronts that constitute the conical sheet $(\xi=\xi_+)$ of the envelope are emitted during the interval $\beta_P^{1/3}<\beta<\beta_P$ of retarded time, while those constituting the second sheet $\xi=\xi_-$ are emitted during $1<\beta<\beta_P^{1/3}$. This may be seen by noting that the intercept of the ξ_- sheet with the $\tilde{z}_P$ axis, the cusp, and the conical apex of the ξ_+ sheet occur at $\zeta=\frac{1}{2}(\beta_P-1)^2$, ζ_c, and 0, respectively, and that, according to Eq. (D8), the values of β at these points are given by 1, $\beta_P^{1/3}$, and β_P, monotonically increasing along the envelope from the ξ_- intercept to the apex.

The particular set of waves that interfere constructively to form the cusp of the envelope, therefore, is different at different observation times: It consists, at a given observation time β_P, of those waves whose emission times lie close to $\beta=\beta_P^{1/3}$. As the observation time β_P changes, so does the emission time of the cusp and hence the identity of the interfering waves in question.

If the source is short lived, then the emission time $\beta=\beta_P^{1/3}$ of a cusp that can be observed at β_P may or may not fall within its life span. The envelope of the emitted waves would be cusped in this case only during a correspondingly short interval of observation time. Figure 9 traces the evolution in time of the relative positions of a particular set of the propagating wave fronts, those emitted during a limited time interval, that were earlier shown in Fig. 7: before their envelope develops a cusp, during the time interval in which their envelope possesses a cusp, and afterward.

In the case of a source whose strength is nonzero only within the finite interval $0<t<T$ of retarded time, for instance, the envelope of the emitted waves has a cusp during the interval of observation time in which $\beta|_{t=0}\leqslant\beta_P^{1/3}\leqslant\beta|_{t=T}$. Solving this for t_P, we obtain

$$M(M^2-1)l/c\leqslant t_P\leqslant M[M^2(1+aT/u)^3-1]l/c, \tag{D12}$$

where $M\equiv u/c$ stands for the Mach number of the source at $t=0$. For $aT/u\ll1$, therefore, the life span of the caustic $3M^2T$ is proportional to that of the source.

The distance of the caustic from the position of the source at the retarded time, i.e.,

$$\overline{R}_P\equiv\overline{R}|_{t=t_P-\overline{R}/c}=\beta_P^{1/3}(\beta_P^{2/3}-1)l, \tag{D13}$$

can be arbitrarily large even when the duration of the source T is short. This is because there is no upper limit on the value of the length l $(\equiv c^2/a)$ that enters Eqs. (D12) and (D13): l tends to infinity for $a\to0$ and is as large as 10^{18} cm when a equals the acceleration of gravity. Thus $\overline{R}_P$ can be rendered

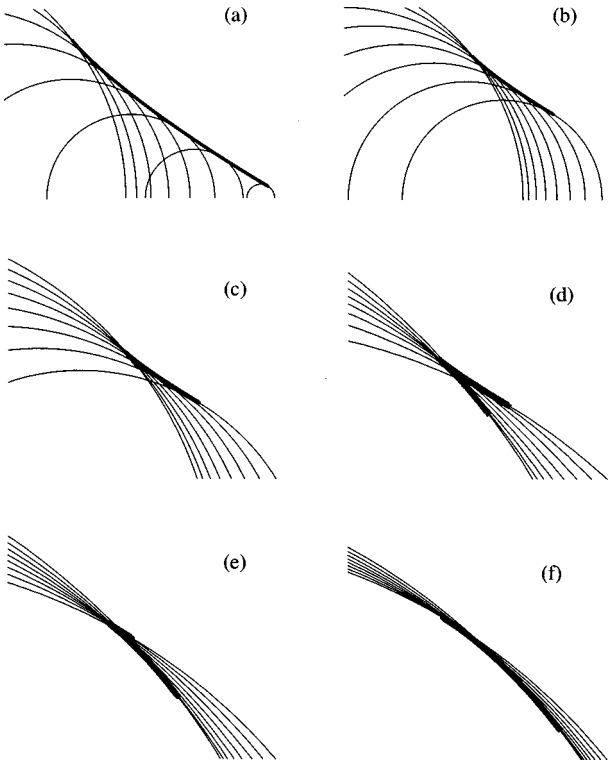

FIG. 9. Evolution in observation time β_P of the relative positions and the envelope of a set of wave fronts emitted during the retarded time interval $1.26<\beta<1.96$. The snapshots (a)–(f) respectively correspond to $\beta_P=2$, 2.5, 3, 3.75, 4.75, and 8. These include times at which the envelope has not yet developed a cusp [(a) and (b)], has a cusp [(c)–(e)], and has already lost its cusp (f).

arbitrarily large, by a suitable choice of the parameter l, without requiring either the duration of the source (T) or the retarded value ($\beta_P^{1/3}c$) of the speed of the source to be correspondingly large.

If either M or l is large, the waves emitted by a short-lived source do not focus to such an extent as to form a cusped envelope until they have traveled a long distance away from the source. The period ($\sim M^2T$) during which they then do so can (in the case of $M\gg 1$) be significantly longer than the life span of the source. (Note that this period is distinct from the duration of the pulse of focused waves that would be received by a stationary observer. The latter is of the order of L_ξ/c, where L_ξ is the dimension of the source in the radial direction.)

For an observation point in the far zone, the two sheets of the truncated envelopes shown in Fig. 9 are essentially coincident. In the vicinity of the cusp, the difference between the dimensionless coordinates ξ_+ and ξ_- of these two sheets at a fixed ζ is given by

$$\xi_+-\xi_-=2(\tfrac{2}{3})^{3/2}\beta_P^{1/3}(\beta_P^{2/3}-1)^{-3/2}(\zeta_c-\zeta)^{3/2}+\cdots \tag{D14}$$

[see Eqs. (D10) and (D11)]. As β_P and hence the distance between the caustic and the source increases, therefore, the separation $(\xi_+-\xi_-)l$ of the two sheets at a finite distance $|\zeta-\zeta_c|l$ from the cusp decreases like $\beta_P^{-2/3}l^{-1/2}$ and so shrinks to zero when either β_P or l is much greater than unity.

The scalar Lienard-Wiechert potential describing the amplitudes of the above waves is given by the retarded solution of the wave equation (14a) for the source density

$$\overline{\rho_0}(x',y',z',t')=\delta(x'-x)\,\delta(y'-y)\,\delta(z'-\tilde{z}-ut'-\tfrac{1}{2}at'^2)\,\theta(t'). \tag{D15}$$

Here the step function $\theta(t)$, which equals 1 when $t>0$ and zero when $t<0$, is introduced to exclude any cases in which the velocity of the source may change direction. In the absence of boundaries, therefore, this potential has the value

$$\overline{G_0}(\mathbf{x}_P,t_P)=2c\int d^3x'\int_{-\infty}^{t_P}dt'\,\overline{\rho_0}(\mathbf{x}',t')\times\delta(|\mathbf{x}_P-\mathbf{x}'|^2-c^2(t_P-t')^2) \tag{D16a}$$

$$=2c\int_0^{t_P}dt'\,\delta(\overline{R}^2(t')-c^2(t_P-t')^2), \tag{D16b}$$

where $\overline{R}(t')$ is the function defined in Eq. (D2) (see, e.g., [12]).

In terms of the variables earlier introduced in Eqs. (D3)–(D7), the expression on the right-hand side of Eq. (D16b) reduces to

$$\overline{G_0}=2l^{-1}\int_M^{\beta_P}d\beta\;\delta(\overline{g})=2l^{-1}\sum_{\beta=\beta_i}|\partial\overline{g}/\partial\beta|^{-1}, \tag{D17}$$

in which the β_i's are solutions of $\overline{g}(\beta)=0$ in the range $M<\beta<\beta_P$. Equation (D17) shows, in conjunction with Fig. 8, that the potential $\overline{G_0}$ of a point source is discontinuous on the envelope of the wave fronts: If we approach the envelope from outside, the sum in Eq. (D17) has only a single term and yields a finite value for $\overline{G_0}$, but if we approach this surface from inside, two of the β_i's coalesce at an extremum of $\overline{g}$ and Eq. (D17) yields a divergent value for $\overline{G_0}$. On the cusp curve of the envelope, where three wave fronts meet tangentially, all three of the β_i's coincide [Fig. 8, curve (b)] and the denominator of the expression in Eq. (D17) both vanishes and has a vanishing derivative ($\partial\overline{g}/\partial\beta=\partial^2\overline{g}/\partial\beta^2=0$).

The uniform asymptotic approximation to $\overline{G_0}$ at points close to this cusp curve can be found by the method outlined in Appendix A. The resulting expressions for the values $\overline{G_0}^{\text{in,out}}$ of this function inside and outside the envelope (or the bifurcation surface) have the same functional forms as those appearing in Eqs. (18) and (19) except that χ, c_1, p_0, and q_0 are respectively replaced by

$$\overline{\chi}=[\overline{g}(\beta_-)+\overline{g}(\beta_+)]/[\overline{g}(\beta_-)-\overline{g}(\beta_+)], \tag{D18}$$

$$\overline{c_1}=(\tfrac{3}{4})^{1/3}[\overline{g}(\beta_+)-\overline{g}(\beta_-)]^{1/3}, \tag{D19}$$

$$\overline{p_0}=\tfrac{1}{2}(\overline{f_0}|_{\nu=\overline{c_1}}+\overline{f_0}|_{\nu=-\overline{c_1}}), \tag{D20}$$

and

$$\overline{q_0}=\tfrac{1}{2}\overline{c_1}^{-1}(\overline{f_0}|_{\nu=\overline{c_1}}-\overline{f_0}|_{\nu=-\overline{c_1}}), \tag{D21}$$

with

$$\overline{f_0}|_{\nu=\pm\overline{c_1}}=\frac{2}{l}\left[\frac{\overline{c}_1\sin\frac{\pi\mp\sigma}{3}}{(\frac{1}{2}\beta_P^2-\zeta+1)\sin\sigma}\right]^{1/2}. \tag{D22}$$

The variable $\overline{\chi}$ equals $+1$ on the sheet ξ_- and -1 on the sheet ξ_+ of the envelope (or the bifurcation surface). In the immediate vicinity of the cusp curve (D11), we have $\beta_\pm \simeq \beta_P^{1/3}\mp(\frac{2}{3})^{1/2}(\zeta_c-\zeta)^{1/2}$ and so

$$\overline{\chi}\simeq(\tfrac{3}{2})^{3/2}\beta_P^{-1/3}(\beta_P^{2/3}-1)[(\beta_P^{2/3}-1)^{1/2}(\xi_c-\xi) -(\zeta_c-\zeta)]/(\zeta_c-\zeta)^{3/2}, \tag{D23}$$

$$\overline{c}_1\simeq\frac{2^{1/2}}{3^{1/6}}\beta_P^{1/9}(\zeta_c-\zeta)^{1/2}, \tag{D24}$$

and

$$\overline{p}_0\simeq\frac{2}{3^{1/3}}l^{-1}\beta_P^{-1/9},\quad \overline{q}_0\simeq-3^{-5/3}l^{-1}\beta_P^{-5/9} \tag{D25}$$

for the leading terms in the expansions of these quantities in powers of $\xi-\xi_c$ and $\zeta-\zeta_c$.

The function $G_0^{\rm out}$ is indeterminate but finite on the envelope [see Eq. (D38)], whereas $\overline{G}_0^{\rm in}$ diverges as $\overline{\chi}\to\pm1$. It can be seen from the expression for $G_0^{\rm in}$ in the immediate vicinity of the cusp curve,

$$\overline{G}_0^{\rm in}\sim\sqrt{3}l^{-1}(\zeta_c-\zeta)^{1/2}\{\beta_P^{2/3}(\zeta_c-\zeta)^3-(\tfrac{3}{2})^3(\beta_P^{2/3}-1)^2 \times[(\beta_P^{2/3}-1)^{1/2}(\xi_c-\xi)-(\zeta_c-\zeta)]^2\}^{-1/2}, \tag{D26}$$

however, that both the singularity on the envelope (at which the quantity inside the curly brackets vanishes) and the singularity at the cusp curve (at which $\xi-\xi_c$ and $\zeta-\zeta_c$ vanish) are integrable singularities. Singularities persist, in other words, only in the physically unrealizable case where a superluminal source is pointlike [1,2].

Let us now consider an *extended* source that moves parallel to the z axis with the constant acceleration a. The density of such a source, when it has a distribution with an unchanging pattern, is given by

$$\overline{\rho}(x,y,z,t)=\overline{\rho}(x,y,\tilde{z})\,\theta(t), \tag{D27}$$

where the Lagrangian variable $\tilde{z}$ is defined by $z-ut-\frac{1}{2}at^2$, as in Eq. (D1), and $\overline{\rho}$ can be any function of $(x,y,\tilde{z})$ that vanishes outside a finite volume.

If we insert this density in the expression for the retarded potential [12] and change the variables of integration from (x,y,z,t) to $(x,y,\tilde{z},t)$, we obtain

$$\overline{A}_0(\mathbf{x}_P,t_P)=2c\int d^3x\int_{-\infty}^{t_P}dt\;\overline{\rho}(\mathbf{x},t)\,\delta(|\mathbf{x}_P-\mathbf{x}|^2 -c^2(t_P-t)^2) \tag{D28a}$$

$$=\int dx\;dy\;d\tilde{z}\;\overline{\rho}(x,y,\tilde{z})\overline{G}_0(x-x_P,y-y_P,\tilde{z}-\tilde{z}_P,t_P), \tag{D28b}$$

where $\overline{G}_0$ is the function defined in Eq. (D17). The potential of the extended source in question at the position $(x_P,y_P,\tilde{z}_P,t_P)$ of a fixed observer is thus given by the superposition of the potentials of the moving source points $(x,y,\tilde{z})$ that constitute it.

Because $\overline{G}_0$ is invariant under the interchange of $(x,y,\tilde{z})$ and $(x_P,y_P,\tilde{z}_P)$ if ζ is at the same time changed to $-\zeta$ [see Eqs. (D3) and (D17)], the locus of singularities of G_0 in the $(x,y,\tilde{z})$ space of source points, i.e., the bifurcation surface of the observer at P, has the same shape as the envelope shown in Fig. 7 but issues from the fixed point $(x_P,y_P,\tilde{z}_P)$ and points in the opposite direction to the envelope (see Fig. 10).

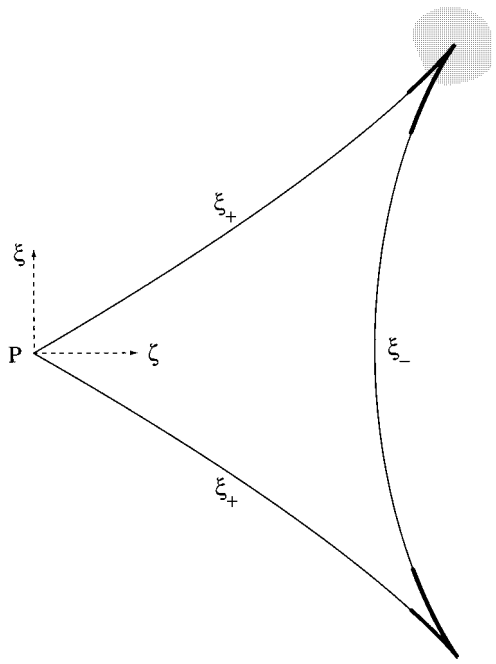

FIG. 10. Cross sections with a meridional plane ($\mu=$const) of the two sheets ($\xi=\xi_\pm$) of the bifurcation surface of the observation point P for $\beta_P=2$. The truncated section of this surface, which is relevant to a short-lived source, is designated by heavier lines. The dotted region represents the volume occupied by the source.

According to Eqs. (D2), (D8), and (D10), the elements inside but adjacent to the bifurcation surface approach the observer along the radiation direction $\mathbf{x}_P-\mathbf{x}$ with the wave speed at the retarded time:

$$\left.\frac{d\overline{R}}{dt}\right|_{\xi=\xi_\pm}=-c. \tag{D29}$$

The accelerations of these elements at the retarded time

$$\left.\frac{d^2\overline{R}}{dt^2}\right|_{\xi=\xi_\pm}=\frac{a(\beta_\mp^3-\beta_P)}{\beta_\mp(\beta_P-\beta_\mp)} \tag{D30}$$

are positive on the sheet $\xi=\xi_+$ of the bifurcation surface and negative on $\xi=\xi_-$ [see the paragraphs following Eq. (D11)]. Hence the source points on the *cusp curve* of the bifurcation

surface, for which $\beta_+=\beta_-=\beta_P^{1/3}$, approach the observer with zero acceleration as well as with the wave speed.

An analysis similar to that presented in Appendix C shows that the ratio $\delta t/\delta t_P$ of emission to reception time intervals for the waves that arise from the source elements on the cusp curve is given by $2^{1/3}(\beta_P^{2/3}-1)^{1/3}(a\,\delta t_P/c)^{-2/3}$. Denoting the wavelength of the radiation by λ and considering the set of waves that are received by the observer with a phase difference $c\,\delta t_P/\lambda$ of only $\frac{1}{2}$, we find that the ratio in question has the value

$$\delta t/\delta t_P \simeq 2(\beta_P^{2/3}-1)^{1/3}(l/\lambda)^{2/3}, \tag{D31}$$

a value that can be exceedingly large: For $\lambda\sim 1$ cm and $a\sim 10^3$ cm/s^2, we have $l/\lambda\sim 10^{18}$, so that this ratio is of the order of 10^{12} even when β_P is not large. Thus the dominant contributions towards the value of the radiation field come from those source elements that approach the observer, along the radiation direction, with the wave speed and zero acceleration at the retarded time.

The preceding discussion applies to a source whose life span encompasses the interval $0<t<t_P$. If the source is short lived, the locus of singularities of G_0 would be modified. We have already seen that when the source has the duration $0<t<T$ the envelope of the wave fronts emanating from one of its elements consists, as in Fig. 9(d), of only a truncated section of the surface shown in Fig. 7 and possesses a cusp during only the correspondingly finite interval of observation time (D12). If we incorporate the finiteness of the duration of the source in the expression for G_0 by replacing the upper limit of integration in Eq. (D28a) with T, then the locus of singularities of the resulting modified G_0 will likewise consist of only a truncated section of the full bifurcation surface, a section such as that designated by the heavier lines in Fig. 10. This locus likewise has a cusp only during the limited interval of time (D12).

For a value of t_P well within the interval (D12), the $\tilde{z}$ extent of the truncated bifurcation surface in question is of the order of $(cT)^2/l$. This can be seen by noting that Eqs. (D8) and (D11) joinly yield the following value for the ζ coordinate of the point of the envelope to which the wave front emitted at the retarded time β is tangential: $\zeta=\zeta_c-(\beta-\beta_P^{1/3})^2(\frac{1}{2}+\beta_P^{1/3}/\beta)$. So, at an observation time close to the center of interval (D12), e.g., for $\beta_P^{1/3}=M+\frac{1}{2}cT/l$, the difference between the ζ coordinates of the cusp and the boundary $\beta=M$ (or $t=0$) of the truncated bifurcation surface is $\zeta_c-\zeta|_{\beta=M}=\frac{3}{8}(1+\frac{1}{3}aT/u)(cT/l)^2$. This expression reduces to $\frac{3}{8}(cT/l)^2$ when $aT/u\ll 1$.

In what follows we let the observation point be such that the cusp curve of the bifurcation surface intersects the source distribution (as in Fig. 10) and designate the portions of the source that fall inside and outside this surface by $V_{\rm in}$ and $V_{\rm out}$. Irrespective of the duration of the source, the separation of the patches of the two sheets of the bifurcation surface that lie within the source is of the order of $\beta_P^{-2/3}l^{-1/2}$ and so is vanishingly small in the far zone [see Eq. (D14)]. The boundaries of the volume $V_{\rm in}$ for a far-field observer consist, therefore, of the surfaces $\xi=\xi_-$, $\xi=\xi_+$, and $\rho=0$ if the source is long lived and of the surfaces $\xi=\xi_-$, $\xi=\xi_+$, and the smaller of $\rho=0$ and $\tilde{z}=\tilde{z}_c-\frac{3}{8}(cT)^2/l$ if the source has the duration T (where $\tilde{z}_c\equiv\tilde{z}_P+\zeta_c l$ is the $\tilde{z}$ coordinate of the cusp).

The gradient of the scalar potential at such an observation point is given, according to Eq. (D28b), by

$$\boldsymbol{\nabla}_P\overline{A}_0=(\boldsymbol{\nabla}_P\overline{A}_0)_{\rm in}+(\boldsymbol{\nabla}_P\overline{A}_0)_{\rm out} \tag{D32}$$

in which

$$(\boldsymbol{\nabla}_P\overline{A}_0)_{\rm in,out}\equiv\int_{\overline{V}_{\rm in,out}} d\overline{V}\,\overline{\rho}\boldsymbol{\nabla}_P\overline{G}_0^{\rm in,out}=-\int_{\overline{V}_{\rm in,out}} d\overline{V}\,\overline{\rho}\boldsymbol{\nabla}\overline{G}_0^{\rm in,out}$$
$$=\int_{\overline{V}_{\rm in,out}} d\overline{V}\,\boldsymbol{\nabla}\overline{\rho}\overline{G}_0^{\rm in,out}-\oint_{\partial\overline{V}_{\rm in,out}}\overline{\rho}\overline{G}_0^{\rm in,out}d\mathbf{S} \tag{D33}$$

and $d\overline{V}$ and $\partial\overline{V}$ stand for the volume element $dx\,dy\,d\tilde{z}$ and the boundary of the volume $\overline{V}$, respectively. Here we have used the fact that $\overline{G}_0^{\rm in,out}$ depend on $(x_P,y_P,\tilde{z}_P)$ in the combinations x_P-x, y_P-y, and $\tilde{z}_P-\tilde{z}$ to rewrite $\boldsymbol{\nabla}_P\overline{G}_0^{\rm in,out}$ as $-\boldsymbol{\nabla}\overline{G}_0^{\rm in,out}$ and have invoked the identity $\rho\boldsymbol{\nabla}G=-G\boldsymbol{\nabla}\rho+\boldsymbol{\nabla}(\rho G)$ and the divergence theorem to arrive at the final expression in Eq. (D33).

We have seen that $\overline{G}_0^{\rm in}$ diverges on the sides $\xi=\xi_+$ and ξ_- of the boundary $\partial\overline{V}_{\rm in}$, but that this singularity of $\overline{G}_0^{\rm in}$ is integrable. Hadamard's finite part of $(\boldsymbol{\nabla}_P\overline{A}_0)_{\rm in}$ consists, therefore, of the volume integral over $\overline{V}_{\rm in}$ in the second line of Eq. (D33). (The contribution from the remaining side of the boundary $\partial\overline{V}_{\rm in}$ that falls within the bifurcation surface vanishes since $\overline{\rho}=0$ on this boundary.)

The function $\overline{G}_0^{\rm in}$ decays like $\overline{p}_0/\overline{c}_1^2=O(\overline{R}_P^{-1/3})$ at points interior to the bifurcation surface [see Eqs. (18), (19), (D24), and (D25)] and the volume $\overline{V}_{\rm in}$, together with the separation of the two sheets of the bifurcation surface, diminishes like $\overline{R}_P^{-2/3}$ [see Eqs. (D13) and (D14)]. It therefore follows that the volume integral in the expression (D33) for $(\boldsymbol{\nabla}_P\overline{A}_0)_{\rm in}$ decays like $\overline{R}_P^{-1/3}\times\overline{R}_P^{-2/3}$ in the far zone. That is to say,

$$\mathcal{F}\{(\boldsymbol{\nabla}_P\overline{A}_0)_{\rm in}\}=O(\overline{R}_P^{-1}),\quad \overline{R}_P/l\gg 1, \tag{D34}$$

a result that can also be inferred from the far-field version of Eq. (D26) by explicit integration. Each component of the volume integral in the expression (D33) for $(\boldsymbol{\nabla}_P\overline{A}_0)_{\rm out}$ has the same structure as the expression for the potential itself and so decays like $\overline{R}_P^{-1}$ [see the paragraph containing Eq. (22)].

To evaluate the surface integral in $(\boldsymbol{\nabla}_P\overline{A}_0)_{\rm out}$ it is more convenient to change the variables of integration from $(x,y,\tilde{z})$ to the dimensionless polar coordinates (ξ,ζ,μ) defined by Eqs. (D4)–(D6) and $\mu\equiv\arctan[(y-y_P)/(x-x_P)]$. Then the elements of area on the sides $\xi=\xi_+(\zeta)$ and $\xi_-(\zeta)$ of the boundary $\partial\overline{V}_{\rm out}$ assume the forms

$$d\mathbf{S}|_{\xi=\xi_\pm(\zeta)}=\mp l^3\xi_\pm d\mu\,d\zeta\,\boldsymbol{\nabla}(\xi-\xi_\pm). \tag{D35}$$

The contribution from the other faces of $\partial\overline{V}_{\rm out}$ to the value of the surface integral in Eq. (D33) is zero, for $\overline{\rho}$ in the inte-

grand of this integral vanishes on the boundary of the source distribution. The surface integral in question can therefore be written as

$$\oint_{\partial V_{\rm out}} \overline{\rho}\overline{G}_0^{\rm out} d\mathbf{S} = \sum_{\pm} \mp l^3 \int_{S_\pm} d\zeta\, d\mu [\xi \overline{\rho}\overline{G}_0^{\rm out}]_{\xi_\pm} \boldsymbol{\nabla}(\xi - \xi_\pm), \tag{D36}$$

in which the patches $S_\pm$ stand for the intersections of the source distribution with the sheets $\xi = \xi_\pm$ of the bifurcation surface, respectively.

Using Eqs. (D8)–(D10), we obtain the following expressions for the vectors normal to these two sheets of the bifurcation surface:

$$\boldsymbol{\nabla}(\xi - \xi_\pm) = l^{-1}[\xi_\pm^{-1}(\tfrac{1}{2}\beta_\mp^2 - \tfrac{1}{2}\beta_P^2 + \zeta)\hat{\mathbf{e}}_z - \hat{\mathbf{e}}_\xi], \tag{D37}$$

where $\hat{\mathbf{e}}_\xi \equiv [(x_P - x)\hat{\mathbf{e}}_x + (y_P - y)\hat{\mathbf{e}}_y]/(l\xi)$ is the radial unit vector pointing away from the path of the source and $(\hat{\mathbf{e}}_x, \hat{\mathbf{e}}_y, \hat{\mathbf{e}}_z)$ are the Cartesian basis vectors.

Furthermore, from Eq. (D18) and an appropriate version of Eq. (19) we find that

$$\overline{G}_0^{\rm out}|_{\xi=\xi_\pm} = \overline{G}_0^{\rm out}|_{\overline{\chi}=\mp 1} \sim (\overline{p}_0 \mp 2\overline{c}_1\overline{q}_0)/(3\overline{c}_1^2), \tag{D38}$$

where we have removed the indeterminacy in the value of $\overline{G}_0^{\rm out}$ at $\overline{\chi} = \pm 1$ by expanding the numerator of Eq. (19) in powers of its denominator and canceling out the common factor $(\overline{\chi}^2 - 1)^{1/2}$ prior to evaluating the ratio in this equation. This shows that $\overline{G}_0^{\rm out}|_{\xi=\xi_-}$ and $\overline{G}_0^{\rm out}|_{\xi=\xi_+}$ remain different even in the limit where the surfaces $\xi = \xi_-$ and ξ_+ coalesce.

Insertion of Eqs. (D37) and (D38) in Eq. (D36) now yields the asymptotic value of the required boundary term in the limit where the observer is located in the far zone and the source is localized about the cusp curve of his or her bifurcation surface. In this limit, the two sheets of the bifurcation surface are essentially coincident throughout the domain of integration in Eq. (D36) [see Eq. (D14)]. So the difference between the values of the source density on these two sheets of the bifurcation surface is negligibly small for a smoothly distributed source and the functions $\overline{\rho}|_{\xi_\pm}$ appearing in the integrand of Eq. (D36) may correspondingly be approximated by their common limiting value $\overline{\rho}_{\rm BS}(\mu, \tilde{z})$ on these coalescing sheets.

Once the functions $\overline{\rho}|_{\xi_\pm}$ are approximated by $\overline{\rho}_{\rm BS}(\mu, \tilde{z})$ and $S_\pm$ are replaced with the surface resulting from the coalescence of these two patches of the bifurcation surface, Eqs. (D37) and (D38) yield an expression for the difference between the two terms in the integrand of Eq. (D36), which reduces to

$$\sum_{\pm} \mp \xi_\pm \boldsymbol{\nabla}(\xi - \xi_\pm)\overline{G}_0^{\rm out}|_{\xi_\pm} \sim \tfrac{1}{3}(\tfrac{2}{3})^{3/2} l^{-2} (\zeta_c - \zeta)^{-1/2} \beta_P^{-2/3} [\xi_c \hat{\mathbf{e}}_\xi - (2\beta_P^{2/3} + 1)\hat{\mathbf{e}}_z] \tag{D39}$$

when it is expanded about $\zeta = \zeta_c$ [see Eqs. (D14) and (D23)–(D25)]. To within the leading order in the far-field approximation $\beta_P \gg 1$, therefore, Eqs. (D36) and (D39) yield

$$\oint_{\partial V_{\rm out}} \overline{\rho}\overline{G}_0^{\rm out} d\mathbf{S} \sim \tfrac{1}{2}(\tfrac{2}{3})^{5/2} \hat{\mathbf{e}}_\xi \beta_P^{-2/3} l^{1/2} \xi_c \int_0^{L_\mu/(\xi_c l)} d\mu \times \int_{\tilde{z}_c - L_{\tilde{z}}}^{\tilde{z}_c} d\tilde{z} (\tilde{z}_c - \tilde{z})^{-1/2} \overline{\rho}_{\rm BS}(\mu, \tilde{z}) \sim (\tfrac{2}{3})^{5/2} \beta_P^{-2/3} L_\mu (L_{\tilde{z}}/l)^{1/2} \langle \overline{\rho}_{\rm BS} \rangle \hat{\mathbf{e}}_\xi, \tag{D40}$$

with

$$\langle \overline{\rho}_{\rm BS} \rangle \equiv \int_0^1 d\hat{\mu} \int_0^1 d\eta\, \overline{\rho}_{\rm BS}|_{\mu = \hat{\mu} L_\mu/(\xi_c l), \tilde{z} = \tilde{z}_c - \eta^2 L_{\tilde{z}}}, \tag{D41}$$

where L_μ is the length of the segment of the cusp curve that falls within the source and $L_{\tilde{z}}$ is given either by the $\tilde{z}$ extent of the intersection of the source distribution with the bifurcation surface or by the smaller of this extent and $\frac{3}{8}(cT)^2/l$; it is given by the former if the source is infinitely long lived and by the latter if the source has a finite life span T.

According to Eq. (D13), the distance between the cusp curve of the bifurcation surface and the observer at the retarded time is $R_P \simeq \beta_P l$ for large values of $\beta_P \equiv (u + at_P)/c$. As the time t_P elapses and the distance between the source and the observer increases, therefore, the value of the above surface integral decays like $\overline{R}_P^{-2/3}$. The second term in the expression (D33) for $(\boldsymbol{\nabla}_P A_0)_{\rm out}$ thus dominates the first term in this equation, which has the conventional rate of decay $\overline{R}_P^{-1}$, and so the quantity $(\boldsymbol{\nabla}_P \overline{A}_0)_{\rm out}$ itself decays like $\overline{R}_P^{-2/3}$ in the far zone $R_P \gg l$.

The electric current density associated with the moving source we have been considering is given by

$$\overline{\mathbf{j}}(\mathbf{x}, t) = c\beta \overline{\rho}(x, y, \tilde{z})\, \theta(t) \hat{\mathbf{e}}_z, \tag{D42}$$

in which $c\beta$ $(\equiv u + at)$ is the velocity of the source pattern at time t. This current satisfies the continuity equation $\partial\overline{\rho}/\partial(ct) + \boldsymbol{\nabla} \cdot \overline{\mathbf{j}} = 0$ in $t > 0$ automatically.

If we insert Eq. (D42) in the expression for the retarded vector potential [12] and change the variables of integration from (x, y, z, t) to $(x, y, \tilde{z}, \beta)$, as in Eq. (D28), we obtain

$$\overline{\mathbf{A}}(\mathbf{x}_P, t_P) = 2 \int d^3x \int_{-\infty}^{t_P} dt\, \overline{\mathbf{j}}(\mathbf{x}, t)\, \delta(|\mathbf{x}_P - \mathbf{x}|^2 - c^2(t_P - t)^2) = \hat{\mathbf{e}}_z \int dx\, dy\, d\tilde{z}\, \overline{\rho}(x, y, \tilde{z}) \times \overline{G}_1(x - x_P, y - y_P, \tilde{z} - \tilde{z}_P, t_P), \tag{D43}$$

in which $\overline{G}_1$ is given by

$$\overline{G}_1 \equiv 2l^{-1} \int_M^{\beta_P} d\beta\, \beta\, \delta(\overline{g}) = 2l^{-1} \sum_{\beta = \beta_i} \beta |\partial\overline{g}/\partial\beta|^{-1}, \tag{D44}$$

and $\bar{g}$ and β_i's are the same quantities as those appearing in Eq. (D17). Application of the method outlined in Appendix A shows that G_1 is described by two different functions $\bar{G}_1^{\rm in}$ and $\bar{G}_1^{\rm out}$ inside and outside the bifurcation surface whose asymptotic values in the neighborhood of the cusp curve have exactly the same functional forms as those of $\bar{G}_0^{\rm in,out}$, the only difference being that $\bar{p}_0$ and $\bar{q}_0$ in these expressions are replaced by $\bar{p}_1$ and $\bar{q}_1$ with the values

$$\bar{p}_1 \simeq \frac{2}{3^{1/3}}\, l^{-1}\beta_P^{2/9}, \quad \bar{q}_1 \simeq \frac{5}{3^{5/3}}\, l^{-1}\beta_P^{-2/9} \tag{D45}$$

in the regime $\tilde{z}_c - \tilde{z} \ll l$ [see Eqs. (18), (19), and (D18)–(D24)].

Hence the following expression for the magnetic field splits into two terms when the observation point is such that the bifurcation surface intersects the source distribution:

$$\bar{\mathbf{B}} = \boldsymbol{\nabla}_P \times \bar{\mathbf{A}} = -\hat{\mathbf{e}}_z \times \int d\bar{V}\, \bar{\rho} \boldsymbol{\nabla}_P \bar{G}_1 . \tag{D46}$$

If we denote the contributions towards the value of $\bar{\mathbf{B}}$ from inside and outside the bifurcation surface by $\mathbf{B}_{\rm in}$ and $\mathbf{B}_{\rm out}$, then for the same reasons as those outlined in the paragraphs following Eq. (D33), it turns out that $\mathbf{B}_{\rm in}$ is divergent and has a Hadamard finite part that decays like $(\bar{p}_1/\bar{c}_1^2)(\xi_+ - \xi_-) = O(\beta_P^{-2/3})$.

Moreover, $\bar{\mathbf{B}}_{\rm out}$ consists of a volume integral with the same structure as the potential and a surface integral of the form $\hat{\mathbf{e}}_z \times \oint_{\partial \bar{V}_{\rm out}} \bar{\rho} \bar{G}_1^{\rm out} d\mathbf{S}$. The volume integral in this case decays like $\beta_P^{-2/3}$ because $\bar{\mathbf{j}}$ is proportional to $\beta_c = \beta_P^{1/3}$ at the retarded time. However, the dominant contribution to the nonspherically diminishing part of $\mathbf{B}$ once again comes from the surface integral in the expression for $\bar{\mathbf{B}}_{\rm out}$.

The evaluation of this surface integral entails precisely the same procedure as that followed in Eqs. (D35)–(D40), except that $\bar{p}_0$ and $\bar{q}_0$ need to be replaced everywhere with $\bar{p}_1$ and $\bar{q}_1$. The outcome of the calculation is

$$\bar{\mathbf{B}} \sim -5\left(\tfrac{2}{3}\right)^{5/2} \beta_P^{-1/3} L_\mu (L_{\tilde{z}}/l)^{1/2} \langle \bar{\rho}_{\rm BS} \rangle \hat{\mathbf{e}}_\mu , \tag{D47}$$

in which $\hat{\mathbf{e}}_\mu = \hat{\mathbf{e}}_z \times \hat{\mathbf{e}}_\xi$ is the unit vector associated with the azimuthal angle $\mu \equiv \arctan[(y - y_P)/(x - x_P)]$.

To find the remaining term $\partial \bar{\mathbf{A}}/\partial t_P = \hat{\mathbf{e}}_z \int d\bar{V}\, \bar{\rho}\, \partial \bar{G}_1/\partial t_P$ in the expression for the electric field, we now need to calculate $\partial \bar{G}_1/\partial t_P$ [see Eq. (D43)]. The Green's function G_1 depends on t_P both through β_P and through $\tilde{z}_P$ and hence ζ. Differentiating the integral representation of $\bar{G}_1$ in Eq. (D44) with respect to these two variables under the integral sign and using the chain rule, we obtain

$$\partial \bar{G}_1/\partial t_P = 4cl^{-2} \int_M^{\beta_P} d\beta\ \beta(\beta - \beta_P)\, \delta'(\bar{g}), \tag{D48}$$

in which use has been made also of Eq. (D3). This can be cast into a form that is more appropriate for integration with respect to the space coordinates by introducing the function

$$\bar{G}_2 \equiv 2l^{-1} \int_M^{\beta_P} d\beta\ \beta(\beta_P - \beta)\, \delta(\bar{g}), \tag{D49}$$

and noting that $\partial \bar{G}_1/\partial t_P = -c(l\xi)^{-1} \partial \bar{G}_2/\partial \xi$ since $\partial \bar{g}/\partial \xi = 2\xi$ according to Eq. (D3).

Once the volume elements $d\bar{V}$ in the above integral representation of $\partial \bar{\mathbf{A}}/\partial t_P$ is written in its polar form $l^3 \xi\, d\xi\, d\mu\, d\zeta$, therefore, we arrive at

$$\partial \bar{\mathbf{A}}/\partial t_P = -cl^2 \hat{\mathbf{e}}_z \int d\xi\, d\mu\, d\zeta\ \bar{\rho} \partial \bar{G}_2/\partial \xi . \tag{D50}$$

This splits into two terms when the observation point is such that the bifurcation surface intersects the source distribution: $\partial \bar{\mathbf{A}}/\partial t_P = (\partial \bar{\mathbf{A}}/\partial t_P)_{\rm in} + (\partial \bar{\mathbf{A}}/\partial t_P)_{\rm out}$ with

$$(\partial \bar{\mathbf{A}}/\partial t_P)_{\rm in} = -cl^2 \hat{\mathbf{e}}_z \int_S d\mu\ d\zeta \int_{\xi_-}^{\xi_+} d\xi\ \bar{\rho} \partial \bar{G}_2^{\rm in}/\partial \xi , \tag{D51}$$

$$(\partial \bar{\mathbf{A}}/\partial t_P)_{\rm out} = -cl^2 \hat{\mathbf{e}}_z \int_S d\mu\ d\zeta \left(\int_0^{\xi_-} + \int_{\xi_+}^{\infty} \right) d\xi\ \bar{\rho} \partial \bar{G}_2^{\rm out}/\partial \xi , \tag{D52}$$

where S is the projection of $\bar{V}_{\rm in}$ onto the (μ,ζ) plane and $\bar{G}_2^{\rm in}$ and $\bar{G}_2^{\rm out}$ differ from $\bar{G}_0^{\rm in}$ and $G_0^{\rm out}$ only in that they entail

$$\bar{p}_2 \simeq \frac{2}{3^{1/3}}\, l^{-1}\beta_P^{5/9}(\beta_P^{2/3} - 1), \quad \bar{q}_2 \simeq 3^{-5/3} l^{-1} \beta_P^{1/9}(5\beta_P^{2/3} - 11) \tag{D53}$$

in place of $\bar{p}_0$ and $\bar{q}_0$.

Integration by parts with respect to ξ shows [20] that the Hadamard finite part of the integral in Eq. (D51) consists of

$$\mathcal{F}\{(\partial \bar{\mathbf{A}}/\partial t_P)_{\rm in}\} = -cl^3 \hat{\mathbf{e}}_z \int_S d\mu\ d\zeta \int_{\xi_-}^{\xi_+} d\xi\ \hat{\mathbf{e}}_\xi \cdot \boldsymbol{\nabla} \bar{\rho} \bar{G}_2^{\rm in} \tag{D54}$$

since the additional boundary term that results from this integration is divergent. In the far zone, this integral has a ξ quadrature that is proportional to $(\bar{p}_2/\bar{c}_1^2)(\xi_+ - \xi_-) = O(\beta_P^{1/3})$ [see Eqs. (D14) and (D19)] and a μ quadrature that is proportional to $L_\mu/(l\xi_c)$ [see Eq. (D41) and the text following it]. Its value decays, therefore, like $\beta_P^{-2/3}$.

The integration by parts with respect to ξ of the right-hand side of Eq. (D52), on the other hand, results in [20]

$$(\partial \bar{\mathbf{A}}/\partial t_P)_{\rm out} = cl^2 \hat{\mathbf{e}}_z \left\{ \int_S d\mu\ d\zeta [\bar{\rho} \bar{G}_2^{\rm out}]_{\xi_-}^{\xi_+} - l \int_{\bar{V}_{\rm out}} d\xi\ d\mu\ d\zeta\ \hat{\mathbf{e}}_\xi \cdot \boldsymbol{\nabla} \bar{\rho} \bar{G}_2^{\rm out} \right\}, \tag{D55}$$

whose terms are both finite. Since for $\beta_P \gg 1$ the retarded value of $\beta_P - \beta$ approximately equals ξ_c [see Eq. (D11)], the volume integral in Eq. (D55) is of the same structure as the expression for the potential $\mathbf{A}$ [cf. Eqs. (D43), (D44), and (D49)] and so decays like $\beta_P^{-2/3}$. However, the surface integral in this expression has a slower rate of decay.

If, as in Eq. (D40), we approximate $\overline{\rho}|_{\pm\xi}$ by $\overline{\rho}_{\rm BS}(\mu,\tilde{z})$, then the relevant version of Eq. (D38) can be used to write the asymptotic value of the surface integral in Eq. (D55) as

$$\begin{aligned}\int_S d\mu\ d\zeta[\overline{\rho}\overline{G}_2^{\rm out}]_{\xi_-}^{\xi_+}&\\ \sim&-\tfrac{5}{2}(\tfrac{2}{3})^{5/2}l^{-3/2}\beta_P^{2/3}\int_0^{L_\mu/(l\xi_c)}d\mu\\ &\times\int_{\tilde{z}_c-L_{\tilde{z}}}^{\tilde{z}_c}d\tilde{z}(\tilde{z}_c-\tilde{z})^{-1/2}\overline{\rho}_{\rm BS}(\mu,\overline{z})\\ \sim&-5(\tfrac{2}{3})^{5/2}l^{-2}\beta_P^{-1/3}L_\mu(L_{\tilde{z}}/l)^{1/2}\langle\overline{\rho}_{\rm BS}\rangle,\end{aligned}\tag{D56}$$

where use has been made of Eqs. (D19), (D53), and (D41). This decays like $\overline{R}_P^{-1/3}$ when $R_P\gg l$ [see Eq. (D13)].

The far-field value of the contribution $(\partial\mathbf{A}/\partial t_P)_{\rm out}$, therefore, consists solely of the boundary term in Eq. (D55) and dominates $\mathcal{F}\{(\partial\overline{\mathbf{A}}/\partial t_P)_{\rm in}\}$, which decays like $\overline{R}_P^{-2/3}$. Moreover, the value thus implied by Eqs. (D51)–(D56) for $\partial\overline{\mathbf{A}}/\partial t_P$ dominates that of $\boldsymbol{\nabla}_P\overline{A}_0$, which also has the decay rate $\overline{R}_P^{-2/3}$ in the far zone [see Eq. (D40) and the text following it].

Thus the electric field vector of the radiation is given by

$$\begin{aligned}\overline{\mathbf{E}}\sim&-c^{-1}\partial\overline{\mathbf{A}}/\partial t_P\\ \sim&-c^{-1}(\partial\overline{\mathbf{A}}/\partial t_P)_{\rm out}\\ \sim&-l^2\hat{\mathbf{e}}_z\int_S d\mu\ d\zeta[\overline{\rho}\overline{G}_2^{\rm out}]_{\xi_-}^{\xi_+}\\ \sim&\overline{\mathbf{B}}\times\hat{\mathbf{e}}_\xi,\end{aligned}\tag{D57}$$

where $\overline{\mathbf{B}}$ is the magnetic field vector given in Eq. (D47). The direction of propagation of the radiation $\hat{\mathbf{e}}_\xi$ is perpendicular to the path of the source, i.e., coincides with the far-field limit of the normal to the envelope of wave fronts at its cusp [see the paragraph following Eq. (D11)]. The polarization vector of the radiation lies along the direction of motion of the source $\hat{\mathbf{e}}_z$.

Note that there has been no contribution toward the values of $\mathbf{E}$ and $\mathbf{B}$ from inside the bifurcation surface. These quantities have arisen in the above calculation solely from the jump discontinuities in the values of the Green's functions $G_0^{\rm out}$, $G_1^{\rm out}$, and $G_2^{\rm out}$ across the coalescing sheets of the bifurcation surface. We would have obtained the same results had we simply excised the vanishingly small volume $\lim_{R_P\to\infty}V_{\rm in}$ from the domains of integration in Eqs. (D33), (D46), and (D50).

The Poynting vector implied by Eqs. (D47) and (D57) is

$$\overline{\mathbf{S}}\sim(\tfrac{5}{3})^2(\tfrac{2}{3})^3\pi^{-1}c\langle\overline{\rho}_{\rm BS}\rangle^2L_\mu^2(L_{\tilde{z}}/l)(\overline{R}_P/l)^{-2/3}\hat{\mathbf{e}}_\xi.\tag{D58}$$

In comparison, the magnitude of the Poynting vector for the *coherent* dipole radiation that would be generated by a macroscopic lump of charge, if it moved subluminally with the constant acceleration a, is of the order of $(\langle\overline{\rho}\rangle L^3)^2a^2/(c^3R_P^2)$, according to the Larmor formula, where L^3 represents the volume of the source and $\langle\overline{\rho}\rangle$ its average density. The intensity of the present emission is therefore greater than that of even a coherent conventional radiation by a factor of the order of $(L_{\tilde{z}}/L)\times(L_\mu/L)^2(l/L)^{5/3}(\overline{R}_P/L)^{4/3}$, a factor that can exceed unity by many orders of magnitude.

Note, finally, that the mechanism responsible for the effect described here remains different from that which gives rise to the Čerenkov effect even in the limit $a\to0$. The electric field (and the electric potential) owing to a rectilinearly moving volume source of infinite duration whose *constant* phase speed exceeds the speed of light *in vacuo* decays nonspherically, but with a different rate $(\overline{R}_P^{-1/2})$ and for a different reason: The emission time interval for those elements of this source that approach the observer with the wave speed at the retarded time is by a factor of the order of $\overline{R}_P^{1/2}/(c\,\delta t_P)^{1/2}$ greater than the time interval δt_P in which the signal generated by them is received. The resulting emission would violate the inverse square law in this case only if the source is infinitely long lived. When the life span of the source in question is finite, both its potential and its field decay spherically, for the contributing interval of retarded time is bounded by the duration of the source.

The present effect, in contrast, comes into play irrespective of whether the duration of the source is finite or infinite and gives rise to a nonspherically decaying caustic (at the distance $\overline{R}_P\simeq\beta_Pc^2/a$ from the source) even in the limit $a\to0$. Here it makes a difference whether we set $a=0$ in Eq. (D1) at the outset or whether we calculate the radiation field for a nonzero acceleration and then proceed to the limit $a\to0$. The envelope of the wave fronts has no cusp in the former case, whereas there is a caustic in the latter case that merely moves to larger distances from the source as $a\to0$ rather than disappear.

[1] B. M. Bolotovskii and V. L. Ginzburg, Sov. Phys. Usp. **15**, 184 (1972).

[2] B. M. Bolotovskii and V. P. Bykov, Sov. Phys. Usp. **33**, 477 (1990).

[3] W. J. Karzas and R. Latter, Phys. Rev. **137**, B1369 (1965).

[4] C. L. Longmire, IEEE Trans. Electromagn. Compat. **20**, 3 (1978).

[5] J. N. Brittingham, J. Appl. Phys. **54**, 1179 (1983); R. W. Ziolkowski, J. Math. Phys. **26**, 861 (1985); P. Hillion, J. Appl. Phys. **60**, 2981 (1986); J. Durnin, J. J. Miceli, and J. H. Eberly, Phys. Rev. Lett. **58**, 1499 (1987); P. L. Overfelt, Phys. Rev. A **44**, 3941 (1991); R. Donnelly and R. W. Ziolkowski, Proc. R. Soc. London, Ser. A **440**, 541 (1993).

[6] V. V. Borisov and A. B. Utkin, J. Phys. A **26**, 4081 (1993); M. R. Palmer and R. Donnelly, J. Math. Phys. **34**, 4007 (1993); V. V. Borisov and A. B. Utkin, *ibid.* **35**, 3624 (1994); P. L. Over-

felt, J. Opt. Soc. Am. A **14**, 1087 (1997). The charges and currents that are considered in these papers, though likewise entailing motion at the wave speed, are distributed over either one or over two dimensions and so require infinitely large densities.

[7] H. Ardavan, Nature (London) **289**, 44 (1981).

[8] A. A. da Costa and F. D. Kahn, Mon. Not. R. Astron. Soc. **215**, 701 (1985).

[9] H. Ardavan, Mon. Not. R. Astron. Soc. **268**, 361 (1994). The material in Sec. 5 of this paper is superseded by the present analysis.

[10] H. Ardavan, J. Fluid Mech. **226**, 33 (1994). Note that the Fresnel condition is essential to the $R_P^{-1/2}$ dependence of the scalar potential considered in this paper. The statement to the contrary in Sec. V of the paper stems from an error: Because the azimuthal separation of the two sheets of the bifurcation surface (here shown in Fig. 6) remains nonzero as $r_P \to \infty$ only at infinitely large distances $\hat{z}_c - \hat{z}$ from the cusp curve, the adopted ranges of integration for the $\hat{z}$ and $\hat{\varphi}$ quadratures in Eq. (70b) of the paper are, in the limit $r_P \to \infty$, inappropriate for a source distribution that has finite extents along the rotation axis and in the azimuthal direction.

[11] M. V. Lowson, J. Sound Vib. **190**, 477 (1996).

[12] J. D. Jackson, *Classical Electrodynamics* (Wiley, New York, 1975).

[13] C. Chester, B. Friedman, and F. Ursell, Proc. Cambridge Philos. Soc. **54**, 599 (1957).

[14] D. Ludwig, Commun. Pure Appl. Math. **19**, 215 (1966).

[15] R. Wong, *Asymptotic Approximations of Integrals* (Academic, Boston, 1989).

[16] R. F. Hoskins, *Generalised Functions* (Horwood, London, 1979); D. S. Jones, *The Theory of Generalised Functions* (Cambridge University Press, Cambridge, 1982); J. Hadamard, *Lectures on Cauchy's Problem* (Yale University Press, New Haven, 1923).

[17] The general theory is normally formulated in terms of the Fourier component $\tilde{G}_0(k) = \int d\nu\, f_0(\nu) \exp[ik(\frac{1}{3}\nu^3 - c_1^2\nu + c_2)]$ of G_0. However, since the highest-frequency contributions towards the value of $\tilde{G}_0(k)$ come from the points at which G_0 is most singular, the uniform approximation that yields the asymptotic value of $\tilde{G}_0(k)$ for large k and small c_1 (i.e., $f_0 \simeq p_0 + q_0\nu$) is the same as that which yields the asymptotic value of G_0 for points close to the locus of its strongest singularity (the cusp curve of the bifurcation surface or of the envelope) and for small c_1. See R. Burridge, SIAM J. Appl. Math. **55**, 390 (1995).

[18] J. H. Hannay, Proc. R. Soc. London, Ser. A **452**, 2351 (1996).

[19] A. Hewish, Mon. Not. R. Astron. Soc. **280**, L27 (1996).

[20] Note that $\partial\overline{\rho}/\partial\xi = (\partial\overline{\rho}/\partial \mathrm{x})(\partial \mathrm{x}/\partial\xi)\mu + (\partial\overline{\rho}/\partial \mathrm{y})(\partial \mathrm{y}/\partial\xi)\mu = -l\hat{\mathbf{e}}\xi \cdot \boldsymbol{\nabla}\overline{\rho}$.